SILICON NANOWIRE ANODE FOR LITHIUM ION BATTERY

by

MD SHAKABUL ISLAM SOURAV (132472)
ASFAQUR RAHMAN (132471)
KAMRUL AHSAN HRIDOY (132470)
RUBYAT RADUAN AHMED (132438)

A Thesis Submitted to the Academic Faculty in Partial Fulfillment of the Requirements for the Degree of

BACHELOR OF SCIENCE IN ELECTRICAL AND ELECTRONIC ENGINEERING

Department of Electrical and Electronic Engineering
Islamic University of Technology (IUT)
Gazipur, Bangladesh

10 November 2017

SILICON NANOWIRE ANODE FOR LITHIUM ION BATTERY

Approved by:

Dr. Syed Iftekhar Ali Supervisor and Associate Professor,
Department of Electrical and Electronic Engineering,
Islamic University of Technology (IUT),
Boardbazar, Gazipur-1704.

Date: 10.11.2017

TABLE OF CONTENTS

LIST OF FIGURES

LIST OF ACRONYMS

LIB	Lithium-Ion Battery
SiNW	Silicon nanowires
NiNP	Nickel nanoparticle
SEM	Scanning electron microscopy
TEM	Transmission electron microscopy
XRD	X-Ray Diffraction
C-coated	Carbon-coated
EC	Ethylene Carbonate
DMC	Dimethyl Carbonate
SEI	Solid Electrolyte Interphase
C rate	Charge rate

ACKNOWLEDGEMENTS

We would first like to thank Almighty Allah, especially my friends, thesis group mates for their tremendous support and patience with me.

We would also like to thank my undergraduate advisor Dr. Syed Iftekher Ali for all of the guidance, insight, and opportunities he has provided for me throughout the whole work. It is truly remarkable to reflect on how much we have learned during the course work.

ABSTRACT

A novel self-supported electrode with long cycling life and high mass loading was developed based on carbon-coated Si nanowires grown in situ on highly conductive and flexible carbon fabric substrates through a nickel-catalyzed one-pot atmospheric pressure chemical vapor deposition. The high-quality carbon coated Si nanowires resulted in high reversible specific capacity (~3500 mA h g−1 at 100 mA g−1), while the three-dimensional electrode's unique architecture leads to a significantly improved robustness and a high degree of electrode stability. An exceptionally long cyclability with a capacity retention of ~66% over 500 cycles at 1.0 A g−1 was achieved. The controllable high mass loading enables an electrode with extremely high areal capacity of ~5.0 mA h cm−2. Such a scalable electrode fabrication technology and the high performance electrodes hold great promise in future practical applications in high energy density lithium-ionbatteries.

CHAPTER 1

INTRODUCTION

The world energy economy is heavily dependent on fossil fuels and nonrenewable sources which are increasingly unsustainable and unfavorable due to a number of reasons. Based on current annual consumption and available fossil fuels, it is estimated the world's fossil fuel resource will be running out in the next 50 to 60 years. The continued increase in demand for oil paradoxically combined the rapid depletion of nonrenewable oil resources is not promising for the future of energy. Combustion of fossil fuels has also caused massive environmental and ecological problems associated by emitting air pollutions (AP) and greenhouse gases (GHG). All these concerns, among others, were sufficient to generate enough interest for cleaner ways to meet our demands through energy storage and conversion without toxic emissions or stress on the environment. The dominant way to store chemical energy and convert it to various forms for human use such as electrical (electric power grid) and kinetic (transportation) is through fossil fuels. In urban centers, human transportation using automobiles is a very significant source of fossil fuel emissions and it dominates the different modes of transportation that exist today. Replacing the internal combustion engine (ICE) with a battery-powered electric motor in electric vehicles (EVs) would enable zero emission transportation. Power systems based on sustainable energy sources instead of burning fossil fuels is also very desirable for the same benefit of minimizing harmful emissions. However, the limitations of current battery technologies have allowed only hybrid electric vehicles (HEVs) and plug-in hybrid electric vehicles (PHEVs) to be widely commercialized. HEVs and PHEVs have both an ICE and a battery-powered electric motor

so it still can release greenhouse gases, but nevertheless the hybrid system enables efficient fuel utilization with reduced emissions.

Renewable energy sources, such as wind and solar, require highly efficient energy storage systems to be able to store and deliver energy on demand to enhance their ability to compete with fossil fuel based energy systems. Lithium (Li) ion batteries are among the most promising candidates for this required improvement in energy storage due to their superior energy density in comparison with other battery chemistries such as nickel metal hydride (NiMH) and lead acid batteries. This is illustrated in Figure 1.

Both gravimetric (per mass) and volumetric (per volume) charge density of lithium ions are superior to all other compounds used in batteries. However there are some bottlenecks that still prevent the large scale commercialization of Li ion batteries for EVs and renewable energy storage, which are hoped to be addressed in this research.

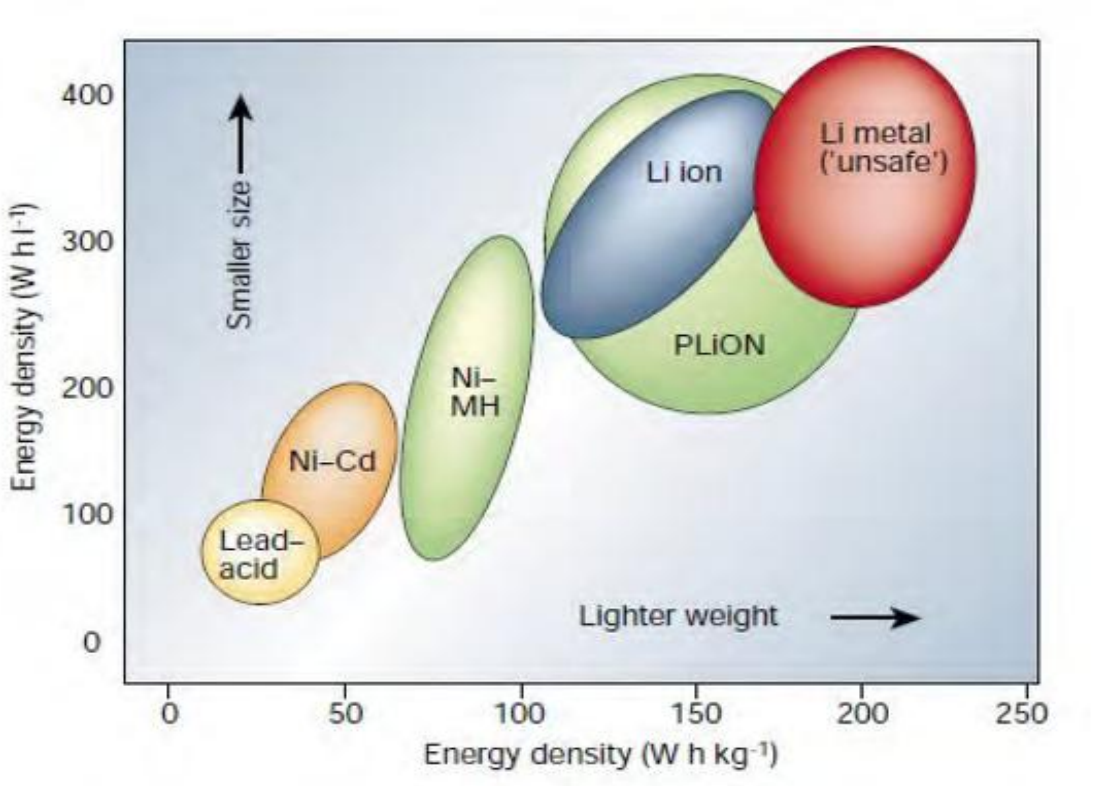

Figure 1: Comparing the energy density of different types of batteries

1.1 OBJECTIVES AND MOTIVATIONS

This project aims to address some of the limitations of commercial LIBs with a novel electrode nanostructure. The first limitation is the limited capacity of the commercially available graphite based LIBs that require massive weights of batteries in order to meet the energy needs of EVs and renewable energy storage. This bolsters the costs of such batteries making commercialization even more difficult. Secondly, safety concerns due to the flammability of both graphite electrodes and the electrolyte at high temperature make it difficult to use for applications where a lot of internal heating occurs, particularly in applications such as EVs.

Despite the improvement of cooling systems and safety mechanisms in laptop computers, for example, companies still issue recalls of batteries due to their safety issues.

Thirdly, they suffer from poor performance at high currents (rate of charge/discharge) which makes them impractical when high power is needed, and this relates to the poor rate capability of the graphite material whereby critical loss in capacity is observed upon significantly increasing the charge/discharge rate of the battery.

Silicon (Si) is a promising replacement to graphite due to its high capacity (4200mAh g-1 theoretical maximum); over ten times that of graphite (372mAhg) and also its stronger resistance to flammability. However, Si suffers from poor stability due to the high volume changes (> 300%) associated with the alloying mechanism in the lithiation of silicon as opposed to the intercalation mechanism in graphite (only 10%). These volume changes cause structural collapse and loss of electrical contact to both the current collector and conductive additives in the composite material leading to rapid capacity decay over subsequent charge/discharge cycles.

Furthermore, silicon is a semiconducting material which, if used without conductive support, suffers from poor capacity and rate capability due to the lack of electrical pathways for charge carriers. Many routes have been investigated to overcome these challenges. Various polymer binders have been demonstrated to be a stabilizing factor helping enhance the structural stability of the Si based electrode through hydrogen bonding with the silicon surface.

Introducing porosity to the silicon material was also found to accommodate the volume changes improving stability of the material, but also reducing the diffusion distance of Li ions allowing for higher charge/discharge rates. Using nanomaterials (such as Si nanoparticles and nanowires) has been found to mitigate propagation of cracks from mechanical stress and hence have inherently higher stability.

Nano-sized silicon materials, such as Si NWs, were found to have shorter Li-ion diffusion distance and hence have higher rate capabilities. However, relying only on faster Li-ion diffusion is not sufficient. The rapid transport of electrons also contributes to the improved rate capability and this was achieved through highly conductive additives such as carbon nanotubes and graphenenano sheets. Furthermore, coating the silicon with a conductive material, such as carbon coating, was found to improve the coulombic efficiency of the silicon-based electrodes because of protecting the silicon active material from direct exposure to the electrolyte.

In this project, a novel electrode nanostructure is proposed whereby silicon nanowires (Si NW) are directly grown on carbon sheets by simple chemical vapor deposition (in atmospheric pressure) with the assistance of Nickel (Ni) nanoparticles (NPs) as a catalyst for growth.

1.2 ORGANIZATION OF THESIS

This thesis which explores the optimal performance achievable with the Carbon Coated SiNW electrode nanostructure is divided into five sections.

Chapter 1, which is this one, introduces the topic with the overview of the objectives of this research and the importance of this work in addressing some limitations of LIBs with a novel electrode nanostructure.

Chapter 2, is intended to provide the necessary background information and literature review of the theory behind the LIB operation, and the properties and synthesis methodologies of Si NWs.

Chapter 3, provides the background information regarding the fabrication process of SiNWs with VLS and Electrical Etching method.

Chapter 4, discusses the Carbon Coated SiNWs generation.

Chapter 5, provides the electrochemical performance of Carbon Coated SiNW anode.

Chapter 6, is the conclusion of this dissertation. Several suggestions and recommendations are proposed for future work, in hopes of developing high capacity, long life silicon anodes for lithium-ion batteries

CHAPTER 2

BACKGROUND INFORMATION

2.1 LITHIUM ION BATTERY PRINCIPLE

Batteries are energy systems that contain one or more electrochemical cells which convert stored chemical energy to electrical energy. Lithium-Ion Battery (LIB) is a class of rechargeable batteries that use lithium reactions in both positive and negative electrodes which can reversibly host and release lithium ions, as illustrated by Figure 2.1 below. Lithium batteries were found to be unsafe due to dendrite formation over the lithium metal after a few cycles that eventually cut through the separators and cause a short-circuit. 4 Lithium-Ion Batteries, on the other hand, use a lithium compound as a cathode material (such as Lithium Cobalt Oxide, shown as Lix-1CoO2 in the figure) which is inherently safer without dendrite formation issues.

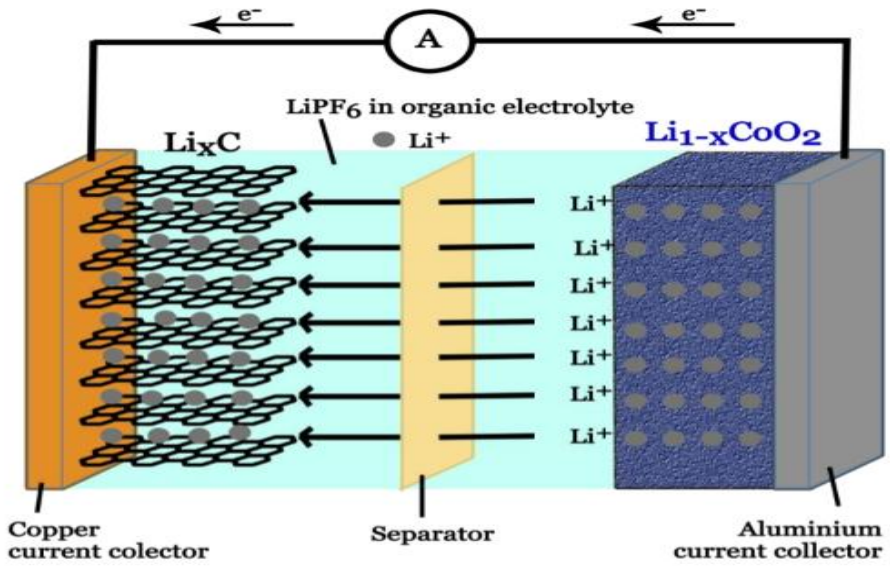

Figure 2.1: Illustration of a common Lithium Ion cell undergoing charge

The most commonly used anode in the LIB industry is a carbon graphite anode (shown as Li_XC in the figure above).

When a cell is manufactured, it is initially at a discharged state with LiCoO2 at the cathode and graphite (C) at the anode. Energy is then stored in the battery by charging it using an external power source.

During charging, as a current is applied through an external power supply, the graphite electrode (C) becomes the cathode (+) where reduction occurs, and the LiCoO2 electrode becomes the anode (-) where oxidation occurs, as illustrated with the redox reactions below:

Reduction at Cathode (+):

$C + x\ Li^+ + x\ e^- = CxLi$

Oxidation at Anode (-):

$LiCoO_2 = Li1\text{-}xCoO_2 + x\ Li+ + x\ e^-$

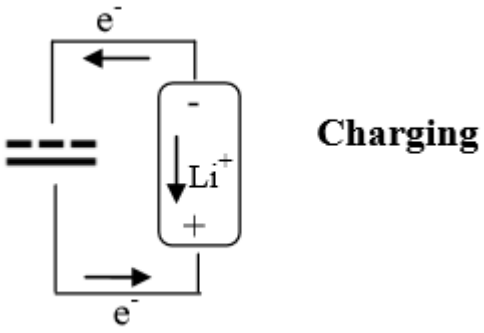

Now the battery is ready to be used as a power source to release the energy stored to a load (such as a light bulb). This time, the $Li1\text{-}xCoO_2$ electrode behaves as the cathode (+) and the lithiated graphite (Li_xC) electrode behaves as the anode (-). (Graphite anode and Lithium cobalt oxide cathode is the naming convention used in the battery industry). The following redox reactions take place when the circuit is closed with a load (e.g. light bulb), leading to current flow:

Reduction at Cathode (+):

$Li_{1-x}\ CoO_2 + x\ Li+ + x\ e^- = LiCoO_2$

Oxidation at Anode (-):

$C_xLi = C + x\ Li+ + x\ e^-$

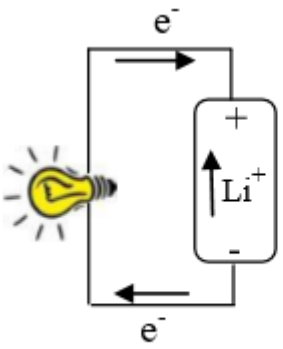

Discharging

What drives the discharge is the electromotive force (EMF) due to the excess electrons found in the unstable lithiated graphite (CxLi) which have a high drive to lose those electrons. In addition, the positive charge generated after the LiCoO2 lose electrons to become Li1-xCoO2 makes it more energetically favorable to gain electrons, and that too has its own EMF. The potential difference across the positive and negative terminals is also known as the EMF. The combined EMF for a typical Li ion battery made from graphite and LiCoO2 is 3.6 V 16, which explains why commercial Li ion cells commonly provide between 3 to 4 V, and a battery made of 4 cells for a laptop computer would provide 12 V.

As the battery is discharged, the potential difference keeps decreasing due to charge neutralization, and the battery is "depleted" when that potential difference reaches zero and the initial state of the material is restored. The battery is then 'recharged' by using an external power supply as done initially to oxidize the LiCoO2 and reduce the graphite and so on and so forth. One cycle is completed after a full charge and discharge are done, and a battery's ability to retain capacity over several cycles is a measure of its stability, also known as capacity retention.

Large loads require more current to be drawn from the battery, and the discharge/charge rate will therefore increase and the battery will deplete faster (smaller time, t). If the capacity of

the battery (relates to the energy, E) does not drop too much after increasing the current drawn, this means it has a high rate capability, and can deliver high amounts of power (P = E/t)

The standard representation of the rate capability of the battery is through the charge rate (C rate). The C rate is based on the time it takes for a full charge to occur, and it can be calculated based on the current applied and maximum reversible capacity. For example, if the reversible capacity of the composite is 2000 mAh/g, then 1C would be a current density of 2000 mA/g, and 0.1C would be 200 mA/g. For 1C at 2000 mA/g it would take 1 hour to reach the maximum capacity (usually less than 1 hour due to the capacity drop associated with increasing the rate), and for 0.1C rate it would take 10 hours to reach the maximum capacity. If the full silicon capacity is considered (4200 mAh/g) then 1 C would be equivalent to 4200 mA/g.

2.2 SILICON NANOWIRES

Silicon nanowires (Si NWs) are cylindrical/wire morphologies of silicon usually below 100 nm in diameter and several μm in length. The first publication of silicon wire growth was by Treuting and Arnold in 1957 17 at a time when they were commonly referred to as ‘silicon whiskers’ or ‘filamentary silicon’ and often much larger than 100 nm in diameter. What features Si NWs can provide for LIBs and the synthesis method will be discussed in the following section.

2.2.1 Si NWS ELECTROCHEMICAL PROPERTIES:

Nanostructured Si materials such as Si NWs and Si NPs have several advantages over bulk Si materials in terms of electrochemical properties. Firstly, the nano-sized diameters have

shorter Li-ion diffusion distance and higher resistance to crack propagation18, allowing for more efficient charge transport and higher mechanical stability (respectively).

The 1D nano-structure of Si NWs is what sets them apart from Si NPs. The advantage can be clearly realized when the direct growth of vertically aligned Si NWs on conductive templates have enabled even higher efficiency of charge transport due to the improved electrical contact and even further reduction of Li-ion diffusion pathways.

2.2.2 SILICON NANOWIRE SYNTHESIS METHOD

There are two main approaches of preparing silicon nanowires: the bottom up approach and the top down approach.

The bottom-up approach, which was the approach first used in history, involves the growth of wires on a nano-sized catalyst (or 'seed') where silicon preferentially deposits and grows in a Chemical Vapor Deposition (CVD) setup. This catalyst is usually a metal nanocrystal on a substrate as per the Vapor-Liquid- mechanisms, but it can also be silicon oxide nucleation cites formed in situ at high temperature as per the Oxide Assisted Growth (OAG) mechanism. The Supercritical Fluid - Liquid - Solid (SFLS) mechanism has also been used which replaces the gas phase with a liquid at supercritical temperature and pressure. This is a solution-based synthesis of SiNWs which is easier to scale up for industrial scale production and hence garnered some research interest.

The top-down approach usually involves the chemical etching of silicon substrates creating void channels that leave behind nanowire morphologies. This is achieved through metal-assisted (electroless) or anodic (electrical) etching with Hydrofluoric Acid (HF). However, this approach involves costly consumption of material and the use of costly and environmentally toxic etchants like HF, and it cannot be used for the direct synthesis of silicon nanowires on graphene and hence does not fit the goal of this research.

2.2.3 ADVANTAGES OF NICKEL (NI) OVER GOLD (AU) IN Li ION BATTERY APPLICATIONS

The most commonly used metal for Si NW growth is gold, Au, because of its high resistance to oxidation and lower temperature required for Si NW growth compared to other metals. Furthermore, the use of Au in the electronics industry has been quite well established with cost effective performance. However, it would be erroneous to assume that the same thing is applicable for the Li-ion battery industry.

In addition to its high cost, gold has been found to be undesirable for the Li-ion batteries due to its capacity loss effect, especially at higher charge/discharge rates, which would work counterproductively with the goal of achieving high rate capability material. This problem can be avoided by adding a gold etching step before using in the battery, but that adds more cost and complication to the process.

On the other hand, nickel (Ni) is a much cheaper material that is commonly used in high performance energy storage devices such as fuel cells, super capacitors and batteries. This also removes the need for any Ni etching steps which would otherwise add more complication and cost to the process.

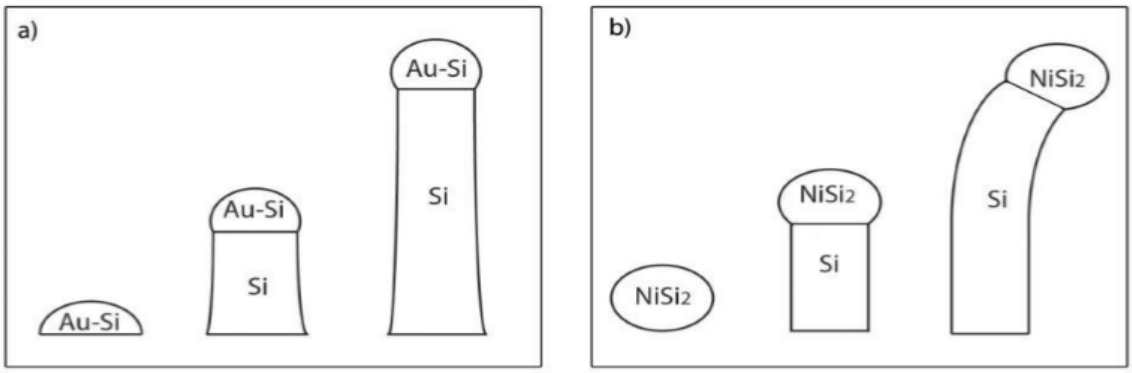

Figure 2.2: Si nanowire growth from a) gold seed undergoing VLS and b) nickel seed undergoing VSS

CHAPTER 3

Si-NW FABRICATION

3.1 SILICON NANOWIRE FABRICATION VIA ELECTROLESS ETCHING

3.1.1 INTRODUCTION

Silicon nanowires can be fabricated and applied as lithium-ion battery anodes, as well as basic building blocks for sensor devices, integrated (nanowire-CMOS) devices, or photovoltaic cells. Electrical contacts between silicon nanowires and metal substrates are essential to nanowire integration and applications. Metal silicides created via metallurgical reactions between silicon and metal are used as electrical contacts for silicon. Among many metal silicides, nickel monosilicide (NiSi), due to its low resistivity as well as low formation temperature and low consumption of silicon, has been widely applied in industrial processes to create low resistance ohmic electrical contacts between planer silicon and substrates.Silicon nanowires are created in an electroless-etching process in aqueous solution, separated from a parent wafer, deposited onto pre-existing nickel inter-digitated electrodes (IDEs) and directly annealed via thermal heating to form silicides. This method allows the facile and low-cost creation of low-resistance ohmic contact between silicon nanowire and

metallic nickel electrodes or substrates. Nanowires with nickel silicides are characterized by electrical resistance measurements, Transmission Electron Microscopy (TEM), X-ray Photoelectron Spectroscopy (XPS) and X-ray Absorption Near Edge Spectrum (XANES) analysis are reported to demonstrate the formation of a nickel monosilicide (NiSi) phase.

3.1.2 SILICON NANOWIRE FABRICATION VIA ELECTRO LESS ETCHING

P-type (boron doped) and n-type (phosphorus doped) single crystal silicon wafer with (100) surface orientation and resistivity of 1-5 Ω·cm were obtained from Montco Silicon Technologies, CA. Silicon wafers were first cleaved and degreased with acetone. Samples were then cleaned via standard wet cleaning procedures including the following steps: de-ionized (DI) water rinse, HF/H2O2/H2O/surfactant ultrasonic cleansing, 1 % HF rinse, and DI water ultrasonic cleansing to remove native oxide and any other surface contamination. Samples were etched in 5.0 M hydrofluoric acid (HF, Aldrich, USA) solutions containing 0.02 M silver nitrate (AgNO3, Fluka, UK) at 50 ºC for a variation of time ranging from 5 minutes to 1 hour. Bulk layer of silver dendrite were removed using 1:1 volume ratio nitric acid solution and followed by 1 % HF dip for 10 seconds to expose the fabricated silicon nanowires. (Note: Silicon nanowires used in the following NiSi formation were p-type and fabricated via 30minutes etch.)

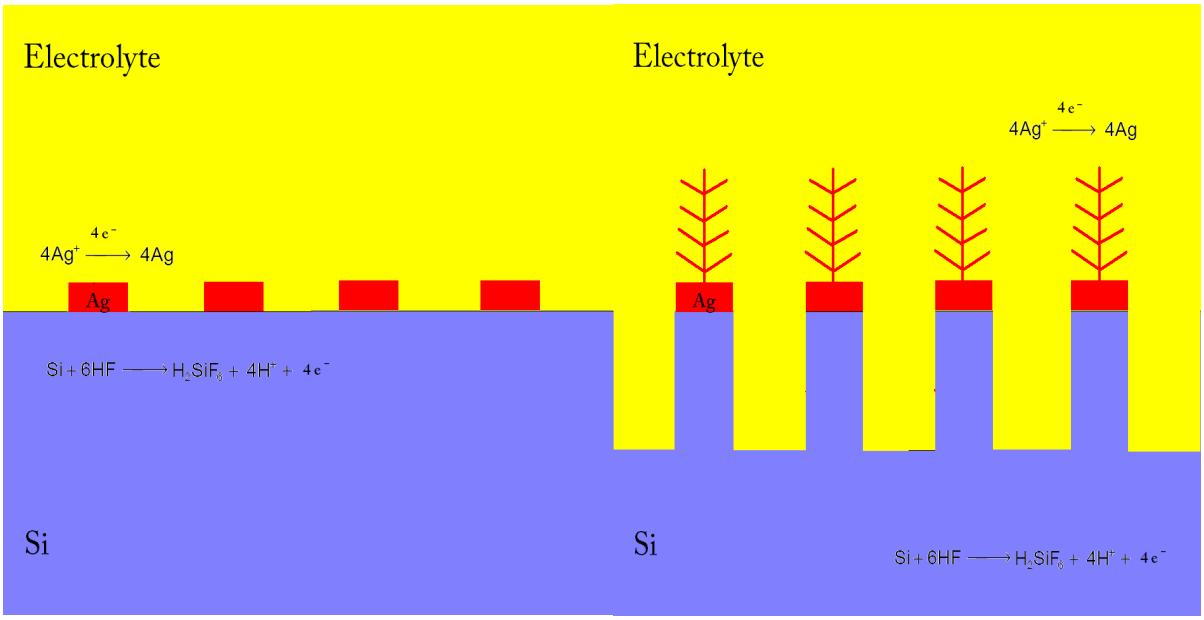

Fig 3.1: Si-NW via Electro less Etching

3.1.3 SILICON NANOWIRE DEPOSITION

The fabricated silicon nanowires were detached from parent substrates via simple mechanical scraping or ultra-sonication and dispersed in transfer solution (e.g. methanol or acetone). These nanowires were then deposited via micropipette on silicon substrate for SEM characterization; Inter-digitated electrodes (IDEs, 3 mm long with 25 comb pairs each, total length 150 mm) with 5 um platinum digit electrode plated with nickel and 5 µm wide spaces were obtained from ABTECH. Silicon nanowires were also deposited on IDEs via micropipette. IDEs deposited with silicon nanowires were dried in argon atmosphere to evaporate transfer solution.

3.1.4 NiSi FORMATION VIA THERMAL ANNEALING

IDEs deposited with silicon nanowires were annealed at 450 ºC for 30 minutes in a reducing atmosphere (Ar: H2 = 4:1 in volume ratio) with fast temperature ramp rate of 10 ºC per minute. In addition to silicidation of nanowires on IDEs, freestanding arrays of nanowires were also used to create silicides for characterization purposes. In this alternative method, a thin (~100 nm) blanket layer of nickel was deposited onto arrays of silicon nanowires attached to the parent substrate via physical vapor deposition or thermal evaporation. These samples were annealed in the same reducing environment for the same duration and excessive nickel was then stripped by wet etching at 40 ºC in commercial thin film nickel etchant (TFGetchant) obtained from Transene.

3.1.5 MATERIAL CHARACTERIZATION

3.1.5.1 SCANNING ELECTRON MICROSCOPY (SEM)

Nanowire morphology and IDE structures were characterized by Scanning Electron Microscope (SEM). The scanning electron microscope (SEM) images the sample surface by scanning it with a high-energy beam of electrons. The electrons interact with the sample and produce signals that contain information about the sample's surface topography. SEM can produce very high-resolution images of a sample surface up to nanometer scale depending on individual SEM system specification (Egerton 2005). Prepared silicon nanowire and IDE samples were attached to SEM sample holder with conductive tape and loaded into SEM chamber to characterization. In this work, a Hitachi S

3600N variable pressure SEM/EDS system was applied. All SEM images were obtained under 15 kV at various amplifications. Silicon nanowire diameters and lengths were measured on screen and converted to true dimensions. A thin layer of gold (~10 Å) was sputtered onto the surface of IDE deposited with silicon nanowires to improve image qualities.

3.1.5.2 TRANSMISSION ELECTRON MICROSCOPY (TEM)

TEM applies a beam of high-energy electrons to transmit through an ultra-thin sample; the electrons interact with sample atoms and then reach to a florescence screen or sensor for imaging. TEM is a useful tool in material characterization and nanotechnology, which can provide nanometer scale high-resolution images for crystal lattices and atomic layer structure, such as crystal orientation and atom position within the specimen. Due to mechanism of TEM imaging technique, samples need to be transparent to incident electrons, and thickness should be in the nanometer scale (Egerton 2005).Transmission Electron Microscope (TEM) was applied to characterize silicon nanowire

withNiSi. The silicon nanowire arrays annealed with nickel were detached from parent substrate in methanol and deposited onto 3840C-FA 200 meshes Lacey Carbon TEM grids (SPI supplies).

A JEOL 2010 high-resolution transmission electron microscopy (HRTEM) was used for characterization. Total time for transferring to TEM chamber was limited to 30 minutes in order to avoid excess native oxide formation on silicon nanowires.

3.1.5.3 X-RAY PHOTOELECTRON SPECTROSCOPY (XPS)

XPS spectra are obtained by irradiating the sample with a beam of X-ray and measuringphotoelectrons escaped from the material. Each element produces a characteristic set of XPS peaks at characteristic binding energy values. A typical XPS spectrum is a plot of the number of electrons detected versus the binding energy of the electrons detected, which directly identify each element that exist in or on the surface of the material being analyzed. XPS is a quantitative spectroscopic analysis tool, providing useful information in determining chemical state of specific species, and quantifying the material composition. XPS analysis has been widely applied to study silicon surfaces and SEI chemical composition (Peled et al. 2001; Bryngelsson et al. 2007; Jung et al. 2007; Chan et al. 2009). XPS characterization for NiSi on silicon nanowires was carried out via a Krato AXIS-165 XPS/Auger surface analysis system. XPS spectra were obtained with Al Kα X-ray source at passing energy of 40 eV. As for depth profiling, Ar+ ion gun was used to sputter the sample surfaces and XPS spectra was obtained at sputtering time at 5, 15, 25, 40 minutes. (Note: Due tothe condition of the XPS system, the sputtering depth corresponding to sputtering time was not identified)

3.1.6 RESULTS AND DISCUSSION (SILICON NANOWIRE FABRICATION)

Silicon nanowires were fabricated via electroless etching of single crystal silicon wafer in aqueous solution as proposed. The nanowires retain the doping and orientation (<100> along the major axis) from the parent substrate. The fabricated silicon nanowires on parent silicon wafer appear in Figure 3.2 as charcoal black due to the large surface area for light absorption.The fabricated nanowires were then detached from parent substrate via mechanical scraping or ultra-sonication and stored in transfer solution (e.g. methanol or ethanol). As can be seen in Figure 3.2, the initially clear solution gradually acquires brownish tinge as silicon nanowires are dissolved into methanol after 2 minutes sonication

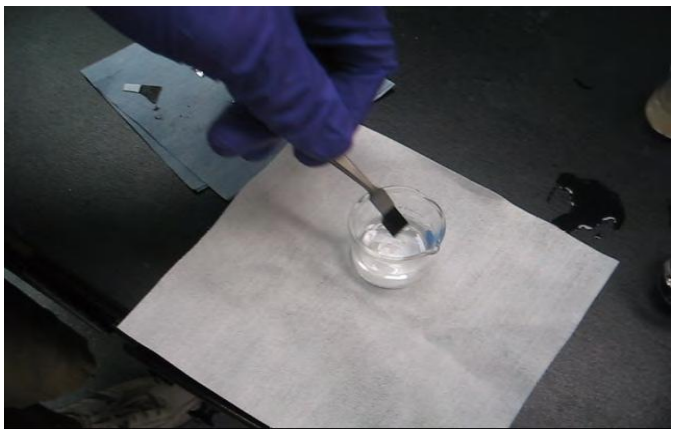

Fig:3.2

Figure 3.3: Optical images of silicon nanowire on parent wafer sample sonicated in methanol for (A) 0 minutes (B) 1 minutes (C) 2 minutes

SEM images of fabricated silicon nanowire vie electroless etching have also been obtained. Figure 3.3 shows a 15-degree titled top-down view SEM image of silicon nanowires fabricated on p-type (100) silicon substrate after 30 minutes etching at 50 ºC. Bundles of silicon nanowire can be clearly observed with residual silver dendrite on top of the nanowire arrays. Piles of detached electrolessly-fabricated silicon nanowires on silicon substrate were observed by SEM as shown in Figure 4.Powder forms of nanowires can also be prepared via centrifuging and drying of the nanowire solution for other applications, such as composite anodes for lithium-ion batteries. The weight of nanowire powders can be measured by precision scale and the average yield of nanowire powders after 30 minutes etch is approximately 1.24 mg · cm-2 as determined by measuring the weight of parent wafer before and after nanowire detachment.

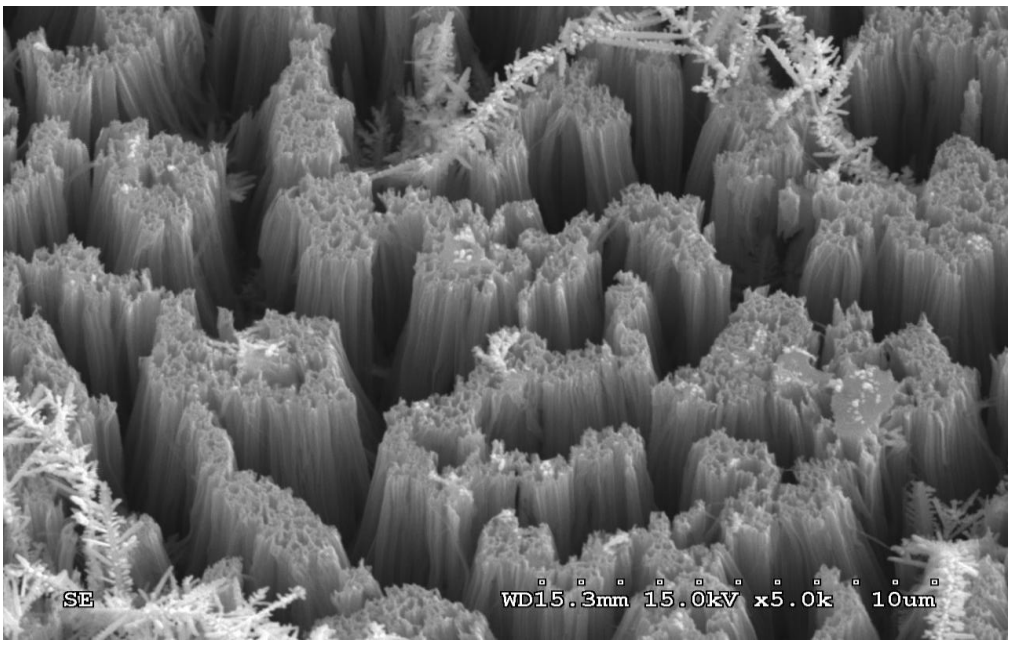

Figure 3.4:Cross-section SEM image of silicon nanowires on p-type silicon wafer via electroless etching for 30 minutes.

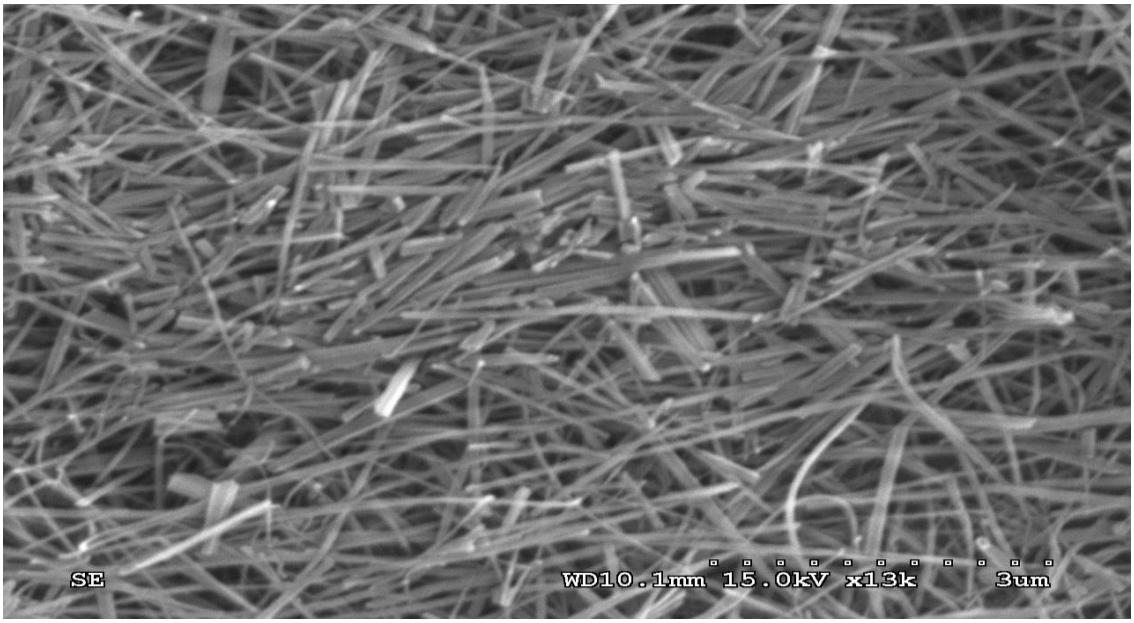

Figure 3.5: SEM image of detached silicon nanowires on substrate.

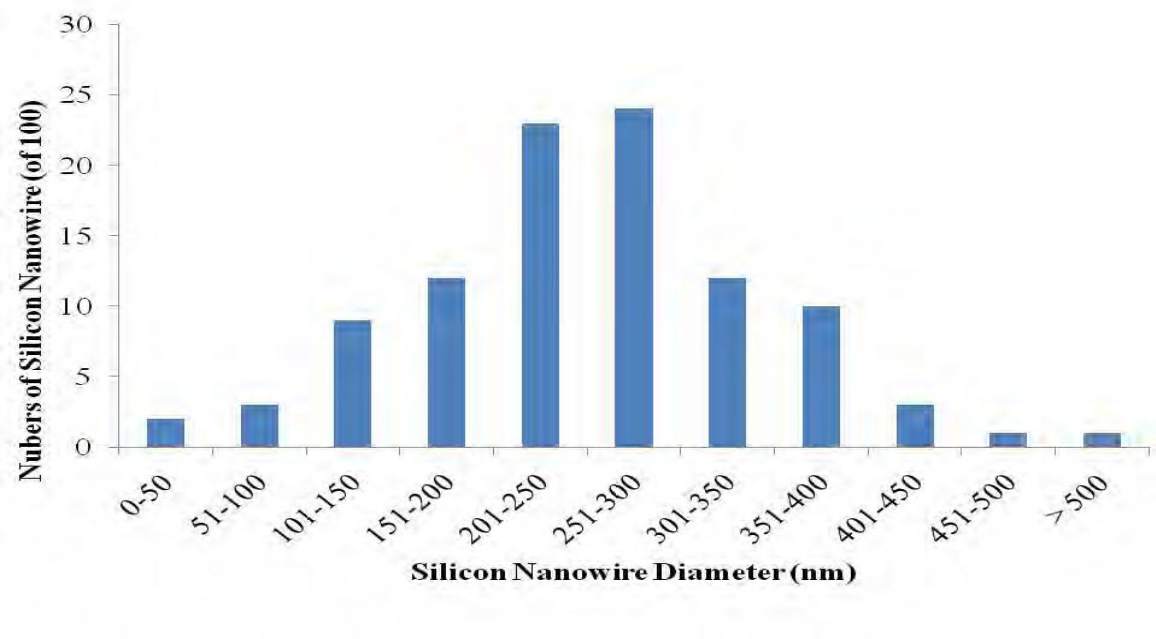

Figure 3.6: Synthesized silicon nanowire diameters distribution.

The diameters of one hundred silicon nanowires have been measured via SEM characterization, and the diameter distribution is ranging from 50 nm to over 500 nm as presented in Figure 3.5. The average silicon nanowire diameter is 253 nm with standard

deviation 1σ for 91 nm. The electroless etching technique is based on the random deposition of silver nano nuclei, and does not have strict control over nanowire diameters compared to other catalytic nanowire growth methods or etching methods with templates.

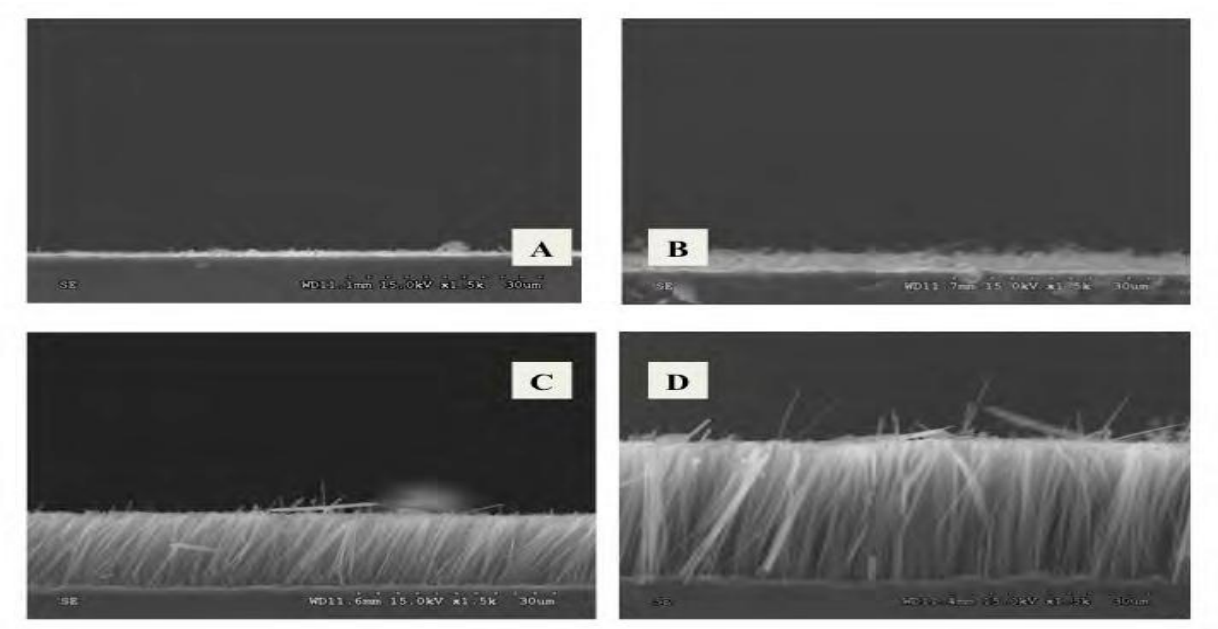

Figure 3.7: Cross-section SEM images of fabricated silicon nanowires on p-type silicon wafers after (A) 5 minutes, (B) 10 minutes, (C) 30 minutes and (D)60 minutes

Silicon nanowires created in the electroless-etching process typically have diameters ranging from 50 to 500 nm and are 10 to 50 μm in length depending on etching time. A 30 minutes electroless etch used to fabricate nanowires for this study resulted in randomly distributed nanowires arrays with lengths in the range of 18-20 μm. Sonication can break nanowire structures and detach nanowires from parent substrates, SEM analysis revealed that separated nanowires are approximately 8-12 μm in length after 2 minutes sonication in acetone or methanol. Some nanowires failed to separate in the sonication procedure resulting in nanowire bundles (< 10 % estimated by SEM analysis).

Silicon nanowires created in the electroless-etching process typically have diameters ranging from 50 to 500 nm and are 10 to 50 μm in length depending on etching time. A 30 minutes electroless etch used to fabricate nanowires for this study resulted in randomly distributed

nanowires arrays with lengths in the range of 18-20 μm. Sonication can break nanowire structures and detach nanowires from parent substrates, SEM analysis revealed that). separated nanowires are approximately 8-12 μm in length after 2 minutes sonication in acetone or methanol. Some nanowires failed to separate in the sonication procedure resulting in nanowire bundles (< 10 % estimated by SEM analysis).

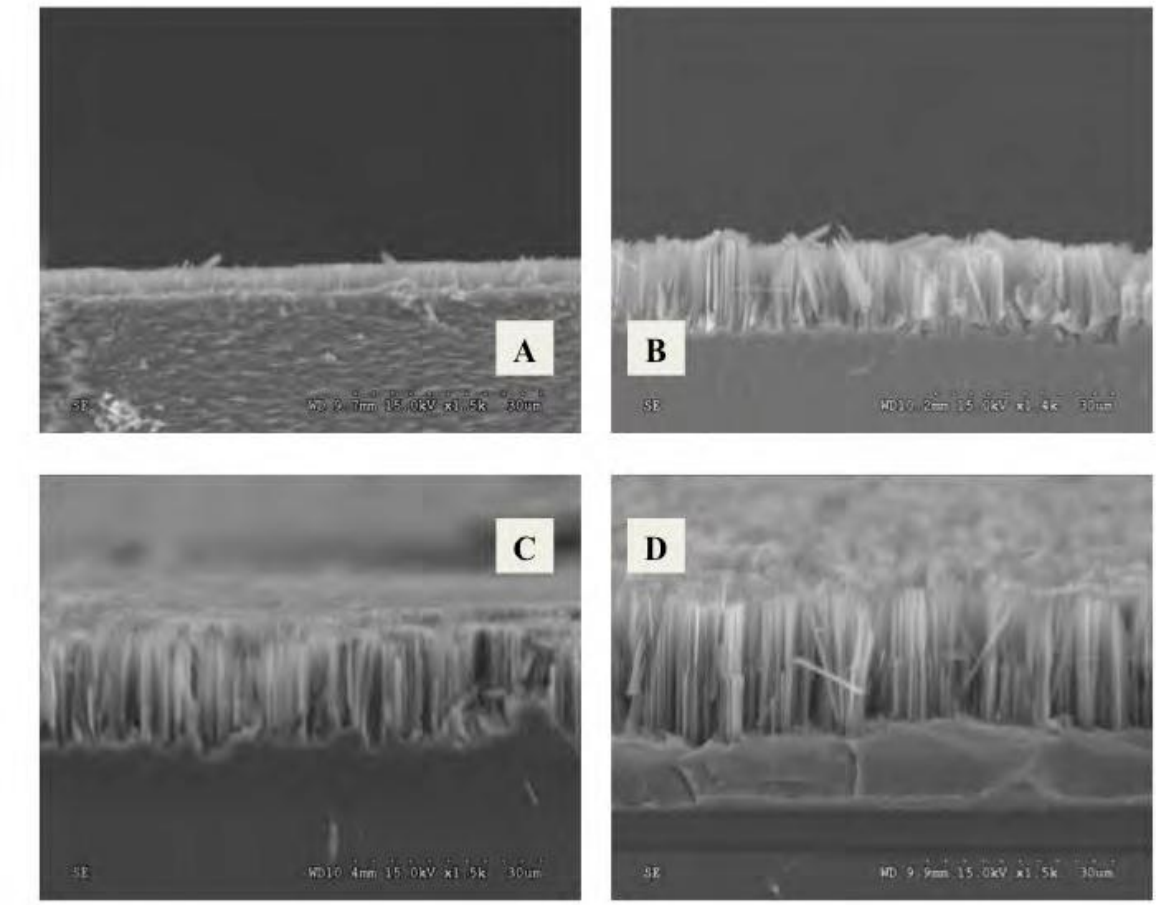

Figure 3.8 Cross-section SEM images of fabricated silicon nanowires on n-type silicon wafers after (A) 5 minutes, (B) 10 minutes, (C) 30 minutes and (D) 60 minutes

To further elucidate the silicon nanowire fabrication via different doping and etching time, both p-type and n-type silicon with (100) surface orientation and 1-5 Ω ・cm resistivity were etched in aqueous solution containing hydrofluoric acid and silver nitrate from 5 minutes to over 1 hour. The cross-section SEM images of 22p-type silicon wafer after 5 minutes, 10

minutes, 30. minutes and 1 hour are presented in Figure 3.7, The cross-section SEM images of n-type silicon wafer after 5 minutes, 10 minutes, 30 minutes and 1 hour are also presented in Figure 3.8. As can be seen from SEM images, the nanowires created on both p-type and n-type silicon substrates show similar structures after electroless etch, and the lengths of silicon nanowire are dependent on etch time.

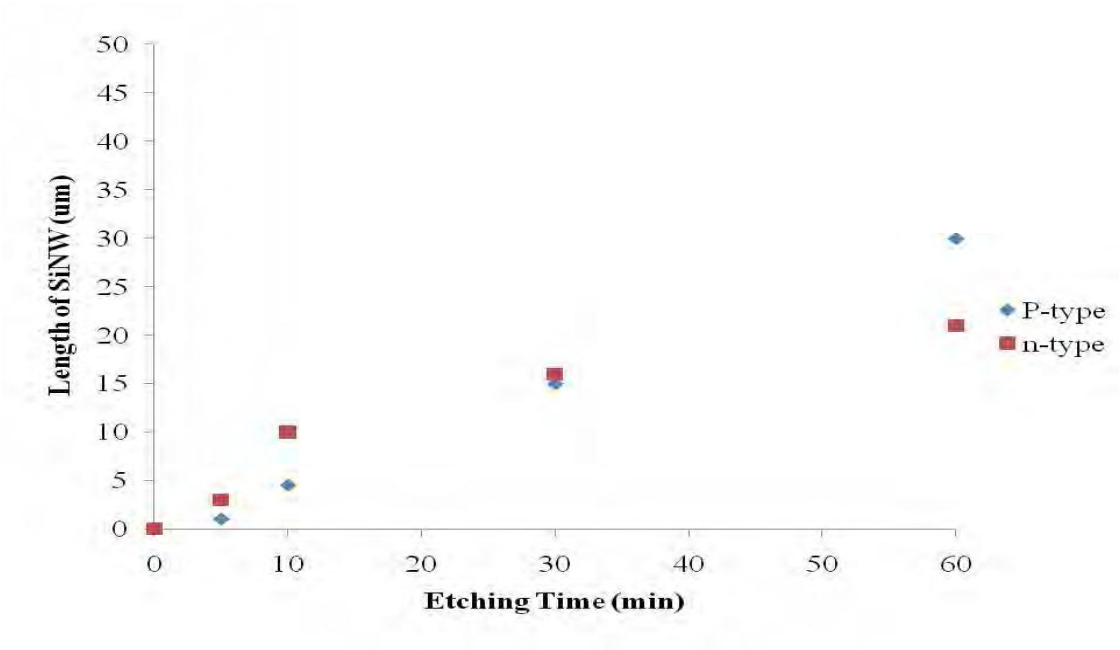

Figure 3.9: Electrolessly fabricated silicon nanowire lengths versus etching time for both p-type and n-type silicon

The nanowire lengths for both p-type and n-type versus etching time were obtained from SEM analysis and plotted in Figure 3.9. The rate for nanowire growth is slightly faster for n-type silicon in the first 10 minutes and gradually slows down and reaches to over 20 μm after 60 minutes etch; while that of p-type silicon is approximately linear. Generally, silicon nanowire structure of 20 μm in length can be obtained after 30 minutes electroless etch at 50 ^{o}C.

3.2 SILICON NANOWIRE FABRICATION VIA VLS METHOD

3.2.1 INTRODUCTION

The **vapor–liquid–solid method** (**VLS**) is a mechanism for the growth of one-dimensional structures, such as nanowires, from chemical vapor deposition. The growth of a crystal through direct adsorption of a gas phase on to a solid surface is generally very slow. The VLS mechanism circumvents this by introducing a catalytic liquid alloy phase which can rapidly adsorb a vapor to super saturation levels, and from which crystal growth can subsequently occur from nucleated seeds at the liquid–solid interface. The physical characteristics of nanowires grown in this manner depend, in a controllable way, upon the size and physical properties of the liquid alloy. Silicon nanowires, also referred to as Si-NWs, are a type of NW most often formed from a Silicon precursor by etching of a solid or through catalyzed growth from a vapor or liquid phase. Initial synthesis is often accompanied by thermal oxidation steps to yield structures of accurately tailored size and morphology. SiNWs have unique properties that are not seen in bulk (three-dimensional) Silicon materials. These properties arise from an unusual quasi one-dimensional electronic structure and are the subject of research across numerous disciplines and applications. The reason that SiNWs are considered as one of the most important one-dimensional materials is they could have a function as building blocks for nano scale electronics assembled without the need for complex and costly fabrication facilities.

3.2.2 EXPERIMENTAL TECHNIQUE:

The VLS process takes place as follows:

1. A thin (~1–10 nm) Au film is deposited onto a silicon (Si) wafer substrate by sputter deposition or thermal evaporation.
2. The wafer is annealed at temperatures higher than the Au-Si eutectic point, creating Au-Si alloy droplets on the wafer surface (the thicker the Au film, the larger the droplets). Mixing Au with Si greatly reduces the melting temperature of the alloy as compared to the alloy constituents. The melting temperature of the Au:Si alloy reaches a minimum (~363 °C) when the ratio of its constituents is 4:1 Au:Si, also known as the Au:Si eutectic point.
3. Lithography techniques can also be used to controllably manipulate the diameter and position of the droplets (and as you will see below, the resultant nanowires).
4. One-dimensional crystalline nanowires are then grown by a liquid metal-alloy droplet-catalyzed chemical or physical vapor deposition process, which takes place in a vacuum deposition system. Au-Si droplets on the surface of the substrate act to lower the activation energy of normal vapor-solid growth. For example, Si can be deposited by means of a $SiCl_4$:H_2 gaseous mixture reaction (chemical vapor deposition), only at temperatures above 800 °C, in normal vapor-solid growth. Moreover, below this temperature almost no Si is deposited on the growth surface. However, Au particles can form Au-Si eutectic droplets at temperatures above 363 °C and adsorb Si from the vapor state (because Au can form a solid-solution with all Si concentrations up to 100%) until reaching a supersaturated state of Si in Au.

Furthermore, nano sized Au-Si droplets have much lower melting points (ref) because the surface area-to-volume ratio is increasing, becoming energetically unfavorable, and nanometer-sized particles act to minimize their surface energy by forming droplets (spheres or half-spheres).

5. Si has a much higher melting point (~1414 °C) than that of the eutectic alloy, therefore Si atoms precipitate out of the supersaturated liquid-alloy droplet at the liquid-alloy/solid-Si interface, and the droplet rises from the surface. This process is illustrated in figure.

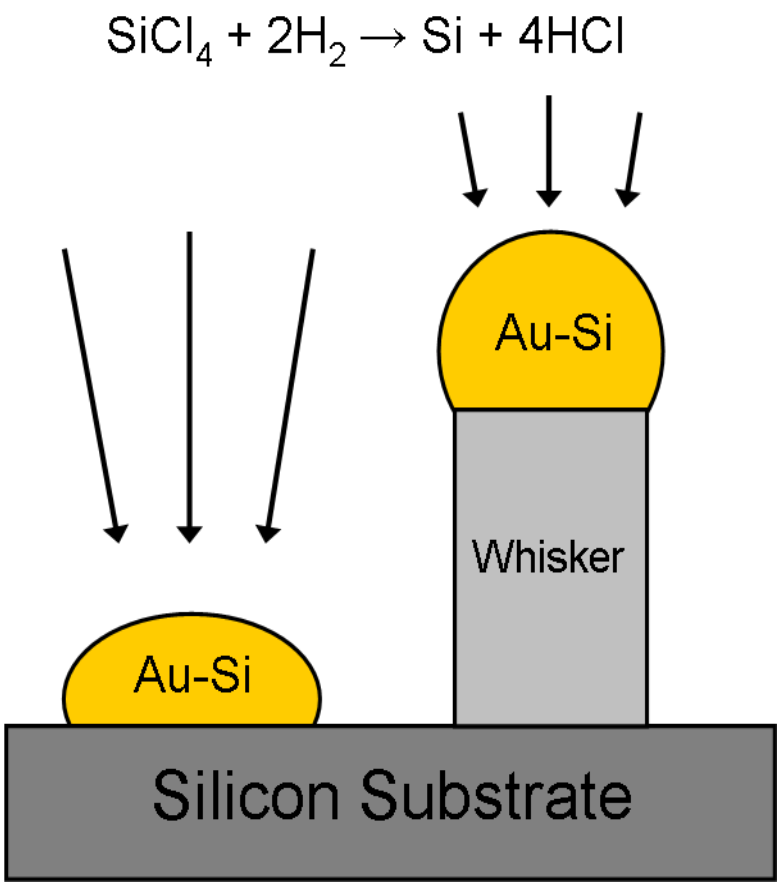

Fig 3.10 : Si NW via VLS method

3.2.3 REQUIREMENTS FOR CATALYST PARTICLES

The requirements for catalysts are:

- It must form a liquid solution with the crystalline material to be grown at the nanowire growth temperature.
- The solid solubility of the catalyzing agent is low in the solid and liquid phases of the substrate material.
- The equilibrium vapor pressure of the catalyst over the liquid alloy must be small so that the droplet does not vaporize, shrink in volume (and therefore radius), and decrease the radius of the growing wire until, ultimately, growth is terminated.
- The catalyst must be inert (non-reacting) to the reaction products (during CVD nanowire growth).
- The vapor–solid, vapor–liquid, and liquid–solid interfacial energies play a key role in the shape of the droplets and therefore must be examined before choosing a suitable catalyst; small contact angles between the droplet and solid are more suitable for large area growth, while large contact angles result in the formation of smaller (decreased radius) whiskers.
- The solid-liquid interface must be well-defined crystallographically in order to produce highly directional growth of nanowires. It is also important to point out that the solid-liquid interface cannot, however, be completely smooth. Furthermore, if the solid liquid interface was atomically smooth, atoms near the interface trying to attach to the solid would have no place to attach to until a new island nucleates (atoms attach at step ledges), leading to an extremely slow growth process. Therefore, “rough” solid surfaces, or surfaces containing a large number of surface atomic steps (ideally 1 atom wide, for

large growth rates) are needed for deposited atoms to attach and nanowire growth to proceed.

3.2.4 METAL-CATALYZED MOLECULAR BEAM EPITAXY

Molecular beam epitaxy (MBE) has been used since 2000 to create high-quality semiconductor wires based on the VLS growth mechanism. However, in metal-catalyzed MBE the metal particles do not catalyze a reaction between precursors but rather adsorb vapor phase particles. This is because the chemical potential of the vapor can be drastically lowered by entering the liquid phase.

MBE is carried out under ultra-high vacuum (UHV) conditions where the mean-free-path (distance between collisions) of source atoms or molecules is on the order of meters. Therefore, evaporated source atoms (from, say, an effusion cell) act as a beam of particles directed towards the substrate. The growth rate of the process is very slow, the deposition conditions are very clean, and as a result four superior capabilities arise, when compared to other deposition methods:

- UHV conditions minimize the amount of oxidation/contamination of the growing structures
- Relatively low growth temperatures prevent inter diffusion (mixing) of nano-sized hetero structures
- Very thin-film analysis techniques can be used in-situ (during growth), such as (RHEED) to monitor the microstructure at the surface of the substrate as well as the chemical composition, using AUG .

CHAPTER 4

CARBON COATED Si-NW ON CARBON FABRIC

4.1 WHY CARBON COATING IS USED?

Silicon holds great promise and has been extensively studied as anode material in both academy and industry owing to its natural abundance and theoretical specific capacity higher than that of graphite (4200 vs 372 mA h g−1) with similar working potential, giving a significantly higher energy density of LIBs.

However, Si suffers from a dramatic volume and structure variation during the Li alloying/dealloying process, resulting in the severe pulverization and delamination from current collectors.

Moreover, the dynamic formation and decomposition of the solid electrolyte interphase (SEI) layer caused by the side reaction between electrolyte and newly exposed Si surface leads to large irreversible capacities and further causes the rapid performance degradation of the Sibased electrodes.

To conquer these critical obstacles, nanostructured Si materials have been widely investigated because they are capable of tolerating extreme changes in volume. Longer nanospheres nanowires nanotubes thin films and various porous or nano-Si/carbon composites than for micrometer-sized Si materials. Particularly, Si nanowire (NWs) has been considered as the most compelling candidate since Zhang's pioneering work and Cui's path-breaking contributions to the development of Si NWs for LIBs. The one-dimensional (1D)

structure provides not only the shorter lithium-ion diff usion distance due to the narrow diameter combined with long continuous paths for electron transport down their length but also a highly porous architecture, allowing volume variation.

4.2 CARBON COATING MECHANISM

The most common approach for the growth of Si NWs involves the medium- or high-pressure chemical vapor deposition (CVD) through the vapor−liquid−solid (VLS) mechanism, where expensive catalysts (e.g., Au, Ag, and Ga) and hazardous materials (e.g., silane) are often applied.

Therefore, advanced technology is highly demanded in the synthesis of high-quality Si NWs for scalable production at low cost.

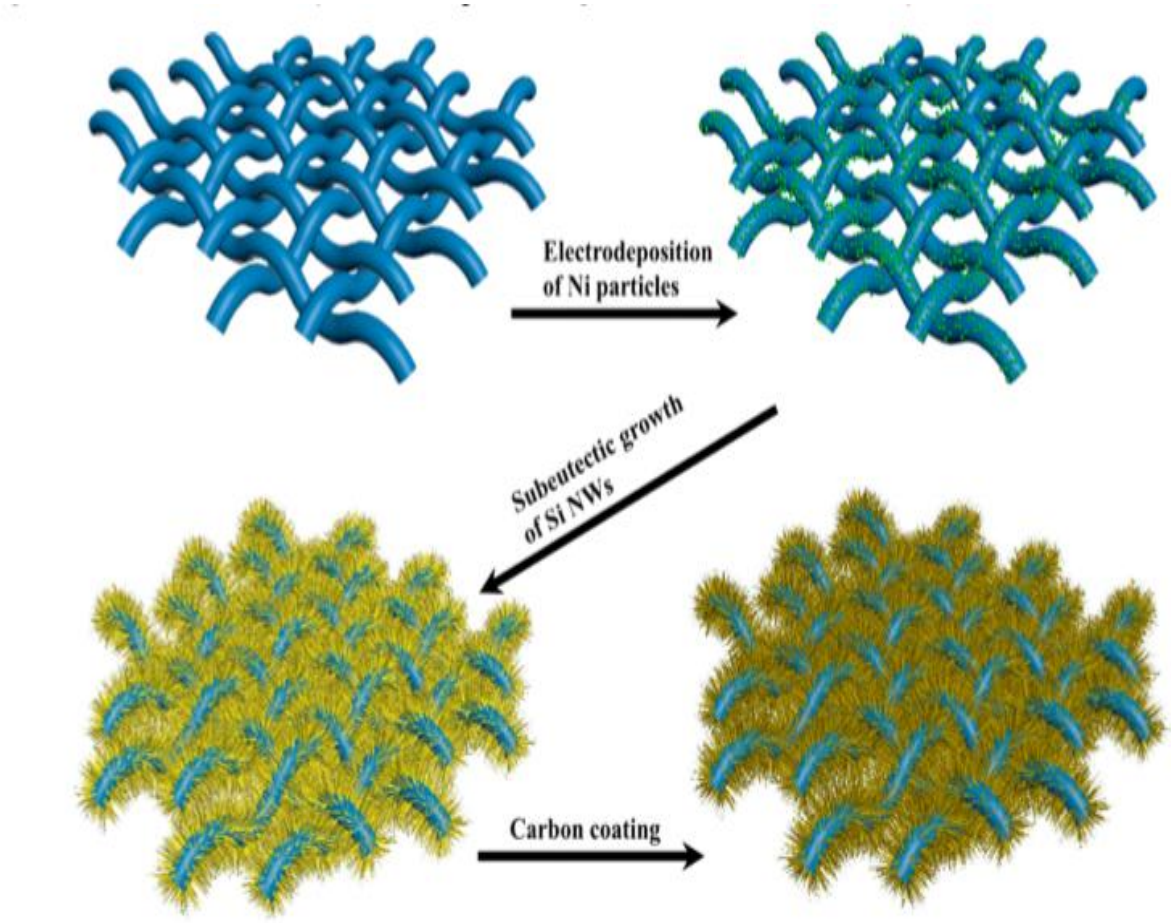

Fig 4.1: Carbon coated Si-NW growth on Carbon cloth

On the other hand, conventional electrode fabrication technology requires significant fractions of binder and conductive agent, which inevitably sacrifice overall energy. Direct deposition of active materials on highly conductive current collectors avoids the use of inert components, resulting in a higher total capacity and a better active material utilization. Moreover, the intimate contact facilitates the electron transport and efficiently improves the electrode integrity as well.The utilization of flexible current collectors enables flexible electrodes, which have been attracting tremendous interest in applications such as wearable electronics and health care devices. So far, there are only a few reports on the fabrication of Si NW-based binder-free and flexible electrodes; however, these flexible electrodes either involve complex synthesis, which is hard for scale-up, or are composed of Si NWs with unsatisfactory quality or nonuniform size. In this context, it is of great importance and challenge as well for effective design and scalable fabrication of high performance flexible Si NW-based electrodes for practical LIB applications.

4.3 SELF-SUPPORTED, FLEXIBLE ELECTRODES:

Herein, we demonstrate self-supported, binder-free, flexible electrodes with long cycling life and controllable high mass loading based on carbon-coated Si NWs grown in situ on highly conductive carbon fabric (CF) substrates (c-Si NWs/CF). The carbon-coated Si NWs are synthesized through a nickel catalyzed, bottom-up growth process via a one-pot atmospheric pressure CVD. Ni nanoparticles are first electro deposite onto a piece of pre cleaned CF before the SiNWs are grown on the Ni catalyst using SiCl4 as the precursor through a vapor−solid−solid mechanism (VSS) at a subeutectic temperature of 900 °C (below the eutectic temperature of 993 °C for Ni−Si system in the VLS growth mechanism).

A thin carbon layer is coated on the Si NWs using toluene as the carbon source, forming a core−shell structure. Such novel electrodes with a unique three-dimensional (3D) architecture possess several characteristics needed for high performance Si-based electrodes. First, the 1D Si NWs and the porous electrode architecture accommodate the volume change well, while the thin-layer carbon coating eff ectively confines the Si NWs during cycling. Second, the in situ growth not only ensures intimate contact of the Si NWs with highly conductive CF, enabling a fast electron transport, but also improves the electrode integrity. Third, high mass loading of carbon-coated Si NWs can be achieved, which holds great potential for next generation LIBs with high areal capacity and energy density.

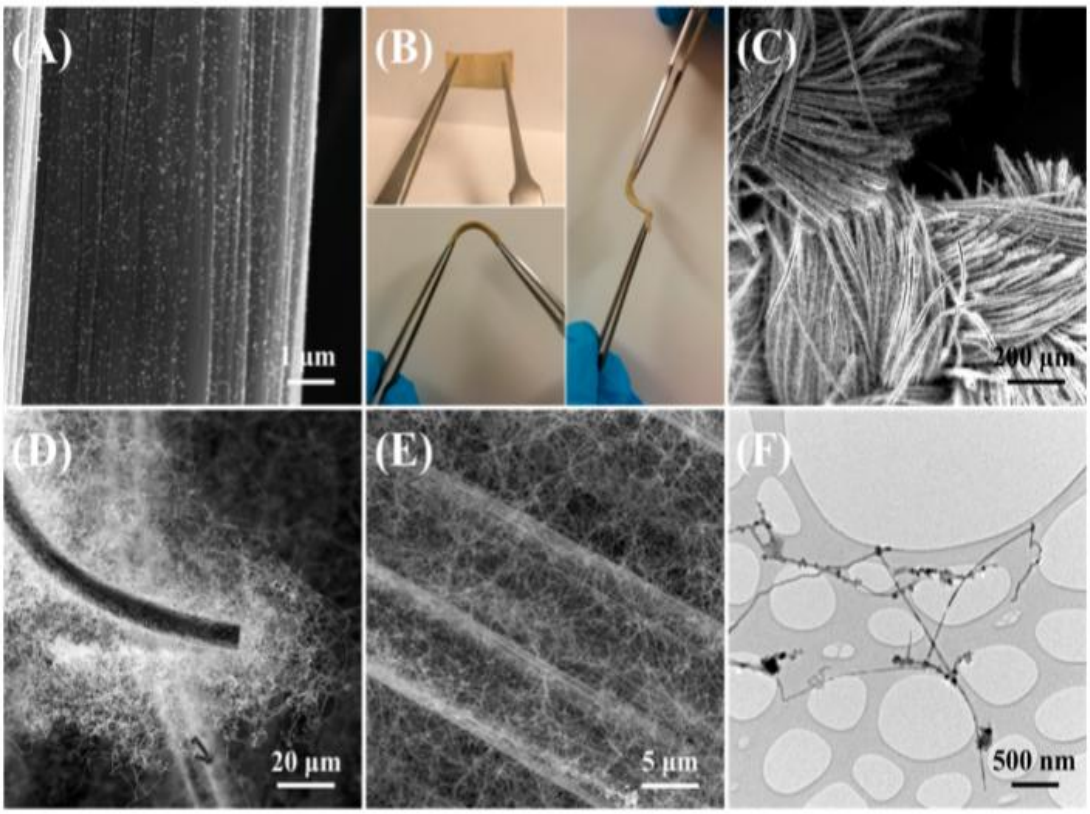

Figure 4.2: (A) Representative SEM image of electrodeposited Ni nanoparticles on carbon cloth. (B) Digital image of the c-Si NWs/CF electrode. (C) Representative SEM image of the c-Si NWs/CF electrode. (D) Low- and (E) high-magnification SEM images of the carbon-

coated Si NWs on the carbon fabric. (F) Representative TEM image of the carbon-coated Si NWs.

Figure 4.2 A shows that the Ni nanoparticles with average size of 20−50 .nm are homogeneously electrodeposited onto carbon fibers from CF After the VSS growth and carbon coating, the as-fabricated c-Si NWs/CF electrodes are binder free and self-supported with high flexibility and robustness (Figure 4.2B) .The mass loading of active materials can be controlled well by tuning the amount of SiCl4 precursor. The morphology of the c-Si NWs/CF electrode was characterized by scanning electron microscopy (SEM). Figure 4.2C displays the well-established architecture of the carbon coated Si NWs grown on the carbon fabric, where the ordered woven structure is fully maintained. These carbon-coated Si NWs homogeneously cover the carbon fibers with a high density from both the tip (Figure 4.2D) and the main body (Figure 4.2E). The representative transmission electron microscopy (TEM) image shows that the 1D NWs possess uniform diameters of approximately 50 nm and lengths of tens of micrometers (Figure 4.2F). Such architecture of the c-Si NWs/ CF electrode is expected to accommodate the volume expansion of Si well and enable a robust electrode, while the high active-surface area and binder-free interface between the Si NWs and CF further benefits the fast ions and electron transfer.

4.4 HIGH-MAGNFICATION TEM IMAGING OF A SINGLE CARBON-COATED SI NANOWIRE

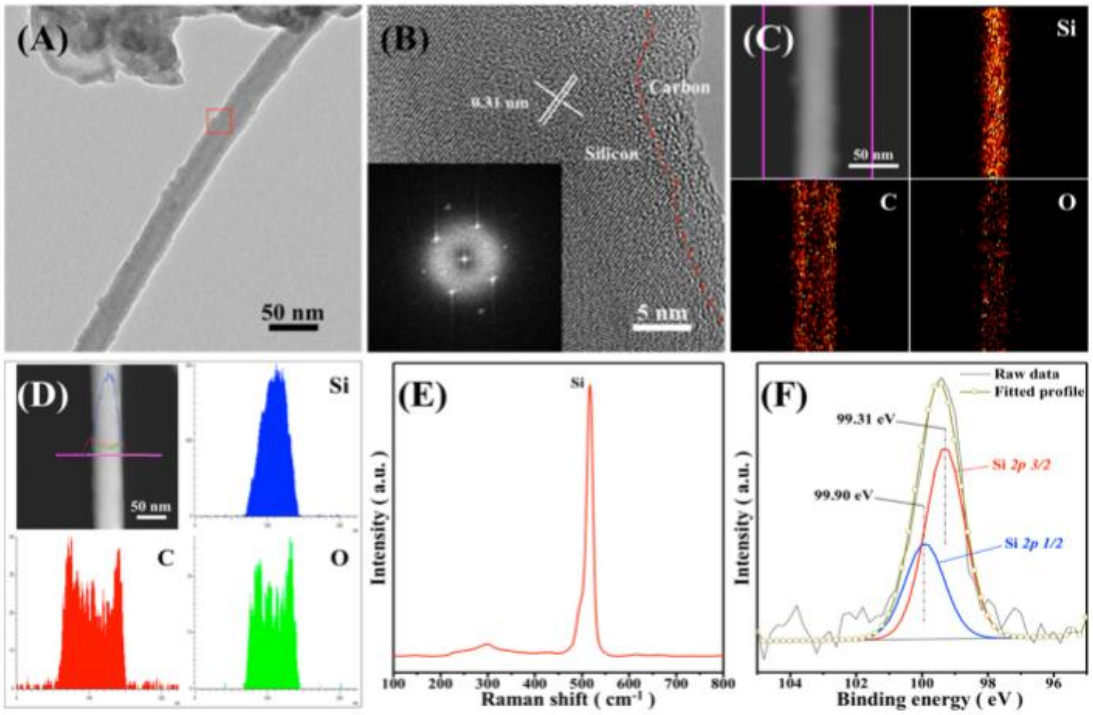

Figure 4.3: (A) CV plots of the c-Si NWs/CF electrode scanned at 0.025 mV s−1 within the voltage window of 1.5 and 0.005 V. (B) Galvanostatic cycling curves of an electrode at the 1st, 2nd, 3rd, 50th, and 100th cycle charged and discharged using 100 mA g−1 within the voltage window of 1.5 and 0.005 V and (C) the corresponding cycling stability. (D) Representative TEM image of a single carbon-coated Si NW after cycling (inset: the high-magnification TEM image of the marked area and the HRTEM image). (E) High-angle annular dark-field STEM (HAADF-STEM) image of the Si NW and corresponding EDX mapping for the marked area. (F) Nyquist plot of the electrode at diff erent cycling statuses at OCV. (G) Longterm cycling behavior of a c-Si NWs/CF electrode cycled using a current of 0.1 A g−1 for 15 cycles and 1.0 A g−1 for another 500 cycles.

Figure 4.3A shows a representative high-magnification TEM image of a single carbon-coated Si nanowire with a diameter of ~34 nm and uniformity along the growth axis. The diameter of the NW matches the size of Ni nanoparticles electrodeposited on the carbon cloth substrate, indicating a Ni catalyzed subeutectic growth mechanism .High-resolution TEM (HRTEM) image of the boxed area marked in Figure 4.3B and the corresponding fast Fourier transform (FFT) diff raction pattern reveal the single crystal characteristic of the Si NWs with a lattice spacing of 0.31 nm, which is consistent with XRD observation and can be indexed to cubic crystal structure .Moreover, a thin layer of amorphous carbon was found with an average thickness of around 3 nm on the surface of the Si NW. Such a core−shell microstructure is further confirmed by energy dispersive X-ray spectroscopy (EDX) mapping (Figure 4.3C) and line-scanning (Figure 4.3D). A small amount of oxygen can also be observed at the interface of the Si NW and carbon layer, which may be ascribed to the impurity of toluene during the coating process, resulting in the mild surface oxidation of Si. The thin-layer carbon coating is intended to provide additional electronic conductivity, prevent the fine Si NWs from further surface oxidation, and also partially restrict expansion during the lithiation process. The existence of Si is also confirmed by Raman spectra (Figure 4.3E), where the strong Si peak can be found at 517 cm−1, while the strong carbon peak is mainly from the carbon fabric substrate (Figure S5). To further analyze the status of Si, XPS was carried out on a c-Si NWs/CF electrode. As displayed in Figure 4.3F, the highly resolved XPS spectra of Si can be interpreted into a doublet at 99.90 and 99.31 eV with a splitting energy of 0.59 eV, which is originated the semicircle correspond to the bulk resistance of the electrolyte, and the resistance of ion migration through the SEI layer, respectively, while the Warburg tail reflects the resistance of ion diff usion in the electrode materials and Structure.

4.5 RESULTS:

During cycling, the semicircle gradually increases, but a relatively low electrode resistance is still retained, indicating a highly robust electrode structure with good electron conductivity and ion diff usivity. To further investigate the superior cycling stability of the c-Si NWs/CF electrodes, the galvano static charge−discharge testing was performed on another electrode at a high current density of 1.0 A g−1 for over 500 cycles after an activation process at 100 mA g−1 for 15 cycles. As shown in Figure 3E, a discharge capacity of 2061 mA hg −1 is achieved after 500 cycles, corresponding to a high capacity retention of 65.9%. In addition to the superior cycling stability, the c-Si NWs/CF electrodes also exhibit good rate capability.. An initial discharge capacity of 4029 mA h g−1 is achieved at 0.1 A g−1 with a high Coulombic efficiency of 87.9%. As the current increases, the cSi NWs/CF electrode still can deliver a capacity of 3236, 2782, and 2138 mA h g−1 at a current of 0.5, 1.0, and 2.0 A g−1, respectively. Even at a high current of 5.0 A g−1, a specific capacity of 1500 mA h g−1 is obtained, corresponding to a capacity retention of 40% when compared with the stabilized capacity at 0.1 mA g−1 . Moreover, a recovery capacity of 3469 mA h g−1 is achieved at 0.1 A g−1, further proving the c-Si NWs/CF electrode is highly robust. The excellent rate capability is mainly ascribed to the small diameter of the Si NWs, which significantly shortens the Li+ diff usion length and provides high surface area for more accessible active sites.

Moreover, the in situ growth and randomly dense packing ensure an intimate contact of the Si NWs with the conductive carbon cloth, which facilitates electron transportation. Practical application of batteries demands electrodes with a high areal capacity, which requires a high loading of active materials on the electrode. However, it is recognized that electrochemical performance strongly depends on the thickness of the electrodes or the loading of active

materials, and the performance generally fades with increased mass loading. Interestingly, our self-supported electrode with unique 3D structure is able to maintain the cycling stability even with extremely high loadings of active materials.

We successfully designed and fabricated self-supported flexible electrodes with long cycling life and high mass loading based on carbon-coated Si nanowires grown in situ on conductive carbon fabric substrates through a one-pot atmospheric pressure CVD process. The high-quality Si nanowires result in high specific capacity, while the unique electrode architecture leads to electrodes with significantly improved robustness and a high degree of electrode stability. The controllable high mass loading enables the electrode with exceptionally high areal capacity. We believe these electrodes hold great promise in future practical applications.

To conquer these critical obstacles, nanostructured Si materials have been widely investigated because they are capable of tolerating extreme changes in volume.12 Longer

cycling performance has been reported for Si nanoparticles, nanospheres, nanowires, nanotubes,thin films, and various porous or nano-Si/carbon composites than for micrometer-sized Si materials.Particularly, Si nanowire (NWs) has been considered as the most compelling candidate since Zhang's pioneering work32 and Cui's18 path-breaking contributions to the development of Si NWs for LIBs. The one-dimensional (1D) structure provides not only the shorter lithium-ion diffusion distance due to the narrow diameter combined with long continuous paths for electron transport down their length but also a highly porous architecture, allowing volume variation. The most common approach for the growth of Si NWs involves the medium- or high-pressure chemical vapor deposition (CVD) through the vapor−liquid−solid (VLS) mechanism, where expensive catalysts (e.g., Au, Ag, and Ga) and hazardous materials (e.g., silane) are often applied. Therefore, advanced technology is highly demanded in the synthesis of high-quality Si NWs for scalable production at low cost.

CHAPTER 5

ELECTROCHEMICAL PERFORMANCE

5.1 INITIAL CHARGE–DISCHARGE PERFORMANCE

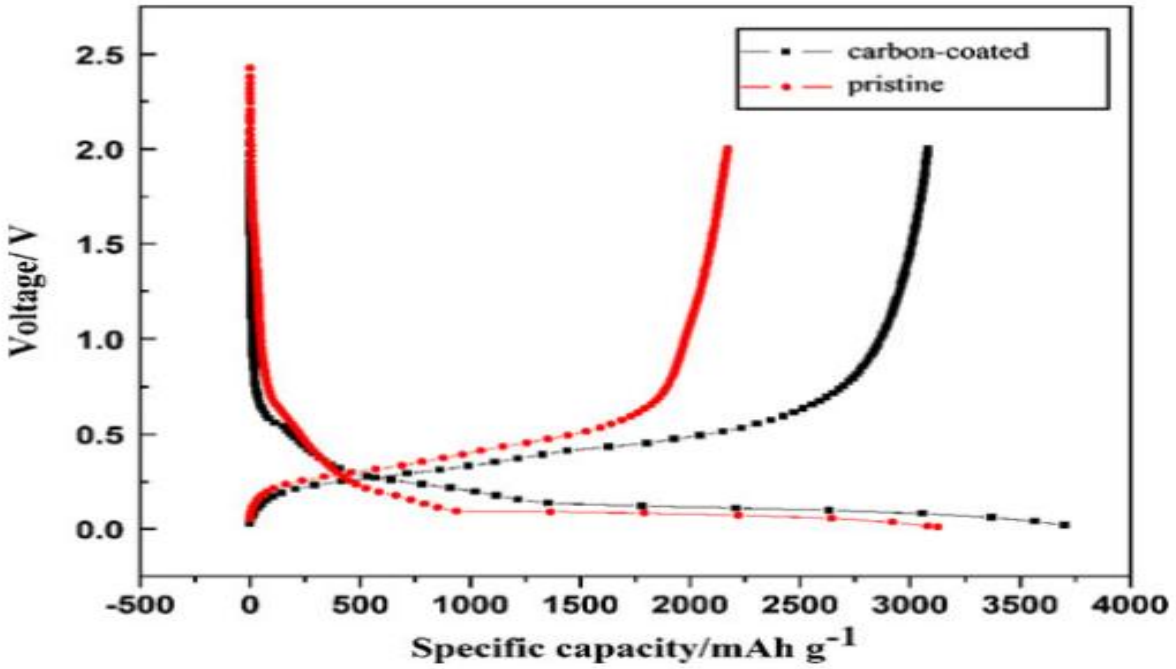

Fig 5.1:Initial charge–discharge curves of the Si NWs with & without carbon coating at 0.05 C rate

Fig. 5.1 shows the initial charge and discharge curves for the Si NWs with and without carbon coating between 0.02 and 2.0 V at acurrent density of 210mAg-1. Theprimary discharge capacity of the Si NWs 38 carboncoating material is 3,125.1 mAhg-1,whereas the chargecapacity is only 2,170.8 mAhg-1,specifying a relatively lowcoloumbic efficiency of 69.5%.The primary dischargecapacity of the carbon-coated Si NWs rises to3,701.8 mAhg-1,

and the charge capacity rises to3,081.6 mAhg-1 that gives a coulombic efficiency of 83.2%.Clearly, the carbon-coated Si NWs material providesmuch higher charge–discharge capacity than that of the SiNWs without carbon-coating. Furthermore, the coulombicefficiency also increases from 69.5% to 83.2%. Here,being certain of that the existence of the carbon layer could resultin the increase of the electronic conductivity and suppressthe reductive decaying of the electrolyte solution onthe surface.

5.2 CYCLING PERFORMANCE OF THE MATERIALS

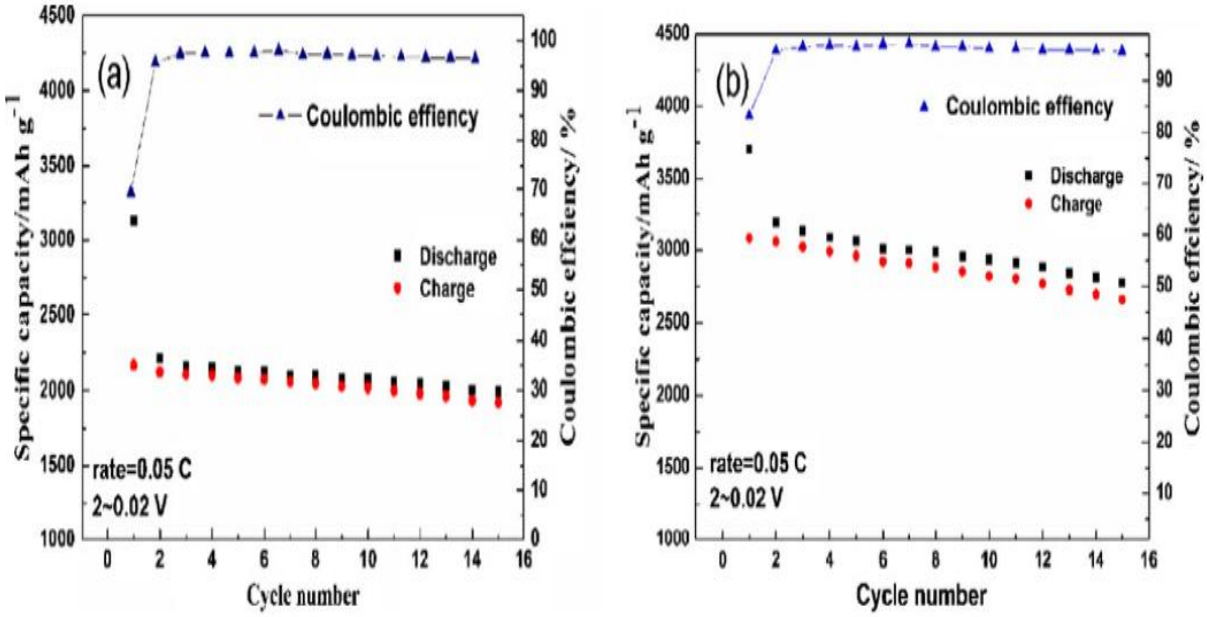

Fig 5.2:Capacity and coulombic efficiency as a function of cycle number for Si NWs with (b) and without (a) carbon at 0.05 C rate

Figure 5.2 shows the capacity and coulombic efficiency as a function of cycle number for Si NWs with and without carbon-coating at 0.05 C (1 C=4,200 mAhg-1) rate. The capacity of the Si NWs without carbon coating falls slowly through charge–discharge cycling and it drops to 1,992.1 mAhg-1 (63.7% of its preliminary discharge capacity) after 15 cycles. Yet, the capacity maintenance ratio of the carbon-coated Si NWs rises to 75% after 15 cycles at

0.05 C. Additionally , the coulombic efficiency of the carbon-coated materials retains above 95% after the main cycle, revealing a good reversibility of the electrochemical reactions. Feyetal reported that TiO2 coating could improve the cyclability of LiCoO2 cathodes, the result was credited to a suppression of the reaction between the cathode surface and the electrolyte and an optimization of the solid electrolyte interphase (SEI) layer . Apparently, the presence of our carbon layer aids the cyclic stability and charge–discharge efficiency of the carbon-coated Si NWs.

5.3 RATE CAPABILITY

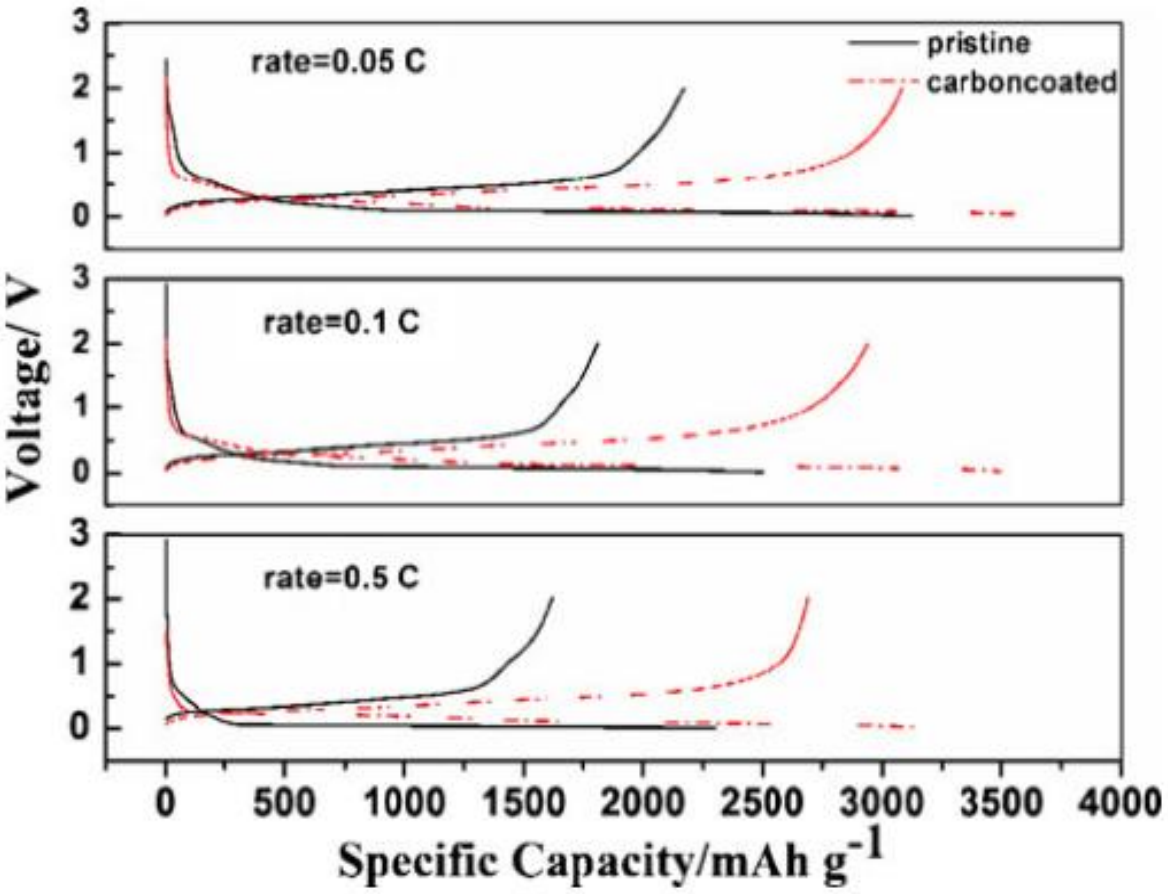

Fig 5.3:Initial charge–discharge curves for the Si NWs with and without carbon coating at 0.05, 0.1, and 0.5 C rate

Figure 5.3 indicates the charge–discharge curves at different rates for 0.05, 0.1, and 0.5 C. We can see that all the carbon-coated Si NWs have higher capacity than the uncoated ones at different rates. The discharge capacities are 3,701.8 mAhg-1at 0.05 C and 3,542.5 mAh g-1at 0.1 C for the coated one. Even at pretty high rate of 0.5 C, the carbon-coated Si NWs can quiet deliver an outstanding capacity of over 3,200.6 mAhg-1 that shows that our materials have good charge–discharge performances. We also studied the cycling performances of the carbon-coated Si NWs material at various current densities as presented in Fig. 9. The discharge capacity holding ratios are about 60% of its preliminary capacity after 30 cycles at all different currents. It is also been demonstrated that the carbon-coated Si NWs material confirms a better cycling performance at various currents compared to the uncoated one.

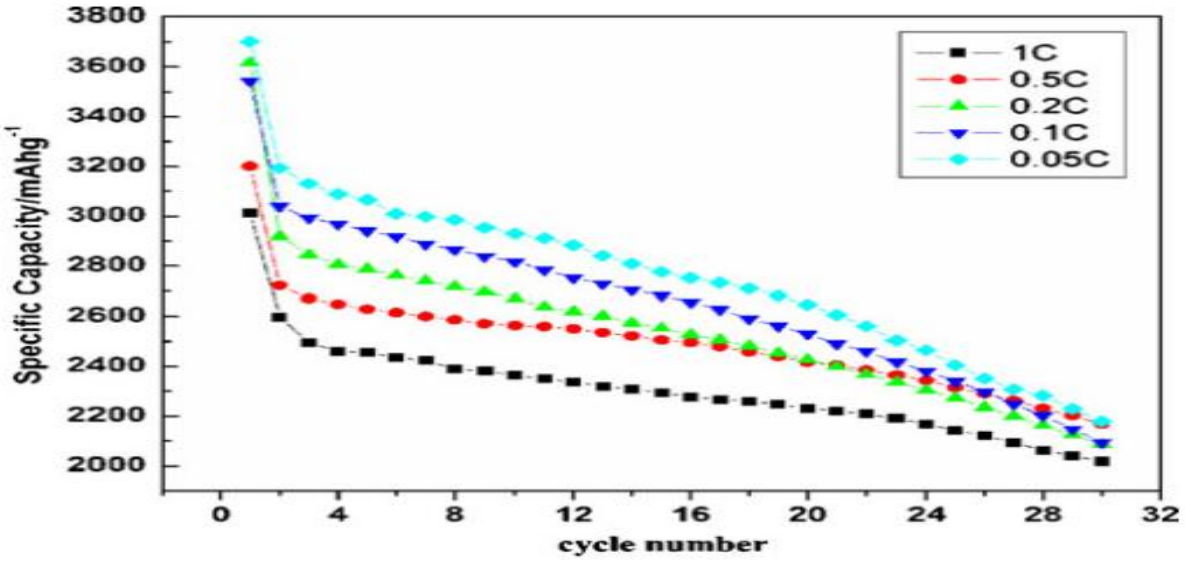

Fig 5.4:Capacity–cycle number curves for Si NWs with carbon coating at 0.05C, 0.1C, 0.2C, 0.5C, and 1C rate

Again,Fig 5.4 shows extended rate capability with continued cycling at 2A/g for 100 cycles compared with the coated(with GRAPHENE) and uncoated SiNWs. This curve shows that at

high current, the capacity of stand-alone graphene or standalone SiNWs are only a fraction of the SiNW-G composite. The rate capability data of the SiNW reference shows much larger capacity drops between each current interval. The Graphene reference shows the lowest capacity drops but also the lowest overall capacity. Overall, the SiNW-G material shows more than 3 times the capacity at high charge/discharge rate which shows the synergestic performance of SiNWs grown on Graphene.The ability to maintain higher capacity despite increasing the current shows that the fast electron mobility required at such high currents is matched with the fast electron mobility possible at the interface between silicon and graphene which is not achievable without the graphene surface.

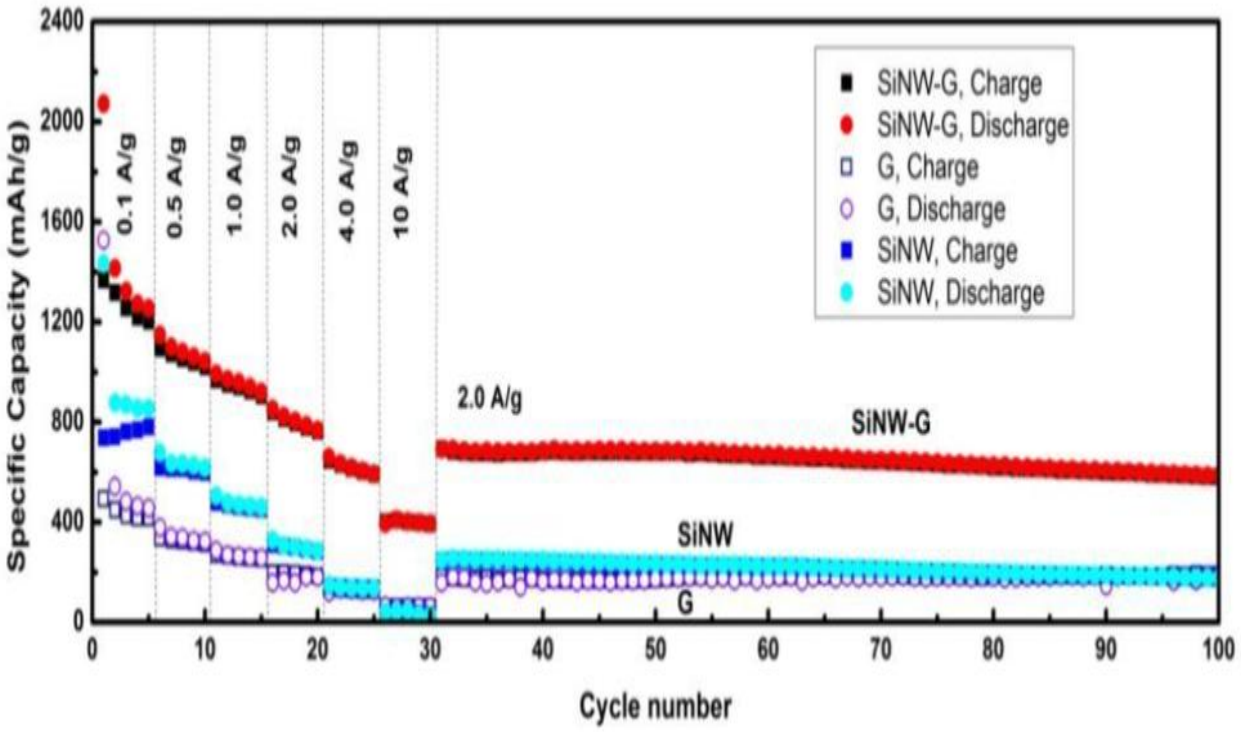

Fig 5.5: Rate capability comparison with SiNW-G, SiNW without G, and G reference

5.4 CYCLIC VOLTAMMETRY

The electrochemical performance of the carbon-coated SiNW film esiselectrode was systematically investigated CV curves of the Si NWs in the initial seven cycles with and without carbon coating between 0.01 and 2.0 V at a scan rate of 0.5 mV s-1 are shown in Fig. 5.5. From the results, a discharge current peak associated with the formation of a solid/electrolyte interface SEI on the surface of the active material. Si alloy began at a potential of about 330 mV and became quite large below 100 mV. In the charging process, current peaks observed at about 370 and 510 mV. The current peak that appeared in the voltage range of 0.5–0.7 V may because of the formation process of SEI layer. The increasing magnitude of the current peaks in cycling may be due to the gradual electrochemical triggering of the electrode in scan. The small peak at150–180 mV may

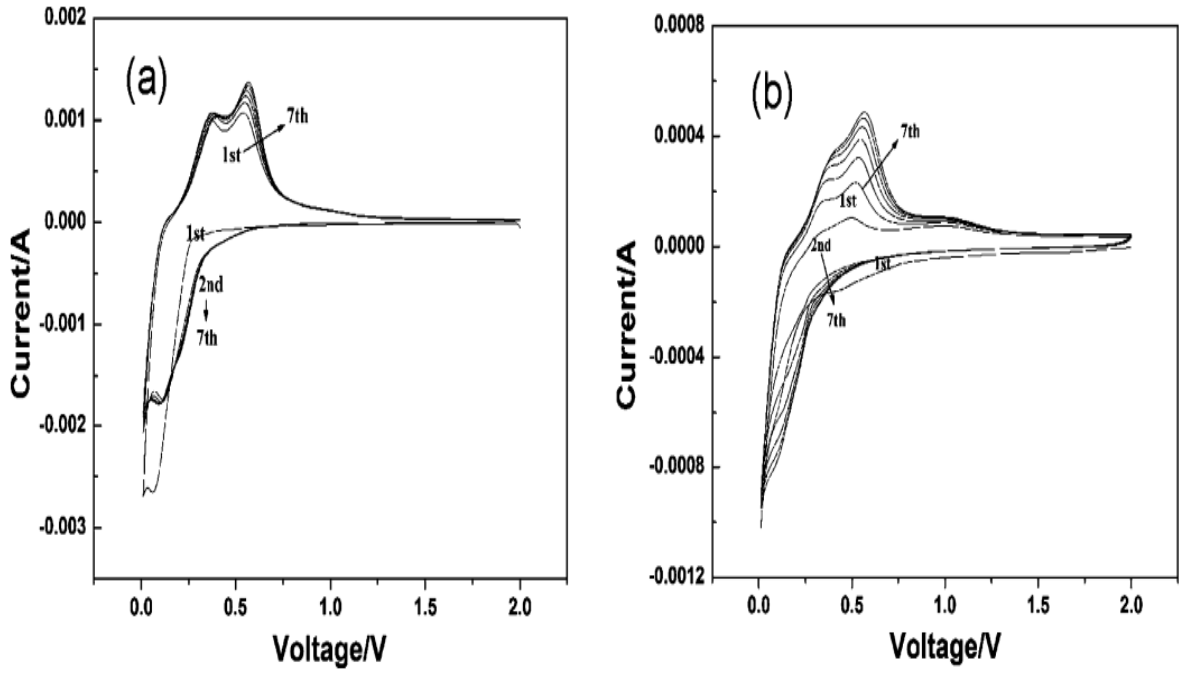

Fig: 5.6

have been produced by the reaction between Li and gold catalyst, which makes a negligible influence to the charge capacity. As a comparison, there are no apparant current peaks relating to SEI layer formation in the voltage range in the first charge of carbon-coated Si NWs material. While the formation of the SEI of the silicon material may arise in the later long cycles, the relative capacity loss contributing to the initial irreversible capacity in the first cycle would be lesser than Si NWs without carbon coating. It supports our assumption that the carbon layercan increase the electronic conductivity and suppress the reductive decomposition of the electrolyte solution on the surface. While the formation of the SEI of the silicon material may arise in the later long cycles, the relative capacity loss contributing to the initial irreversible capacity in the first cycle would be lesser than Si NWs without carbon coating. It supports our assumption that the carbon layercan increase the electronic conductivity and suppress the reductive decomposition of the electrolyte solution on the surface.

CHAPTER 6

SUMMARY AND FUTURE WORK

The first electrode composition studied was to see the effect of controlling the SiNWs content, and it was found that too high SiNW amount (above 70 wt%) had higher capacity but very low stability, and too low SiNW content (below 30 wt%) showed superior stability but very lowcapacity. It was recommended to use 50 wt% SiNW (including Ni mass) with 50 wt% carbon support as a good compromise to achieve good capacity with good stability.

In conclusion, we successfully designed and fabricated self supported flexible electrodes with long cycling life and high mass loading based on carbon-coated Si nanowires grown in situ on conductive carbon fabric substrates through a one-pot atmospheric pressure CVD process. The high-quality nanowires result in high specific capacity, while the unique electrode architecture leads to electrodes with significantly improved robustness and a high degree of electrode stability. The controllable high mass loading enables the electrode with exceptionally high areal capacity. We believe these electrodes hold great promise in future practical applications.

6.1 RECOMMENDATION FOR FUTURE WORK

Further optimize the material and electrode composition to further improve the long range stability in the order of 500-5000 cycles to be compatible with industrial life time specifications.

.

REFERENCES

[1] Scrosati, B. and J. Garche, Lithium batteries: Status, prospects and future. Journal of Power Sources, 2010. 195(9): p. 2419-2430.

[2] Divya, K.C. and J. Østergaard, Battery energy storage technology for power systems—An overview. Electric Power Systems Research, 2009. 79(4): p. 511-520..

[3] Díaz-González, F., et al., A review of energy storage technologies for wind power applications. Renewable and Sustainable Energy Reviews, 2012. 16(4): p. 2154-2171.

[4] Tarascon, J.-M. and M. Armand, Issues and challenges facing rechargeable lithium batteries. Nature, 2007. 414: p. 359-367.

[5] Goodenough, J.B. and Y. Kim, Challenges for rechargeable batteries. Journal of Power Sources, 2011. 196(16): p. 6688-6694.

[6] Lenovo customer support. Battery recall. 2014 [cited 2014 April 7]; Available from: http://support.lenovo.com/en_US/detail.page?DocID=HF004122

[7] Sivakkumar, S.R., J.Y. Nerkar, and A.G. Pandolfo, Rate capability of graphite materials as negative electrodes. ElectrochimicaActa, 2010. 55(9): p. 3330-3335

[8] Kasavajjula, U., C. Wang, and A.J. Appleby, Nano- and bulk-silicon-based insertion anodes for lithium-ion secondary cells. Journal of Power Sources, 2007. 163(2): p. 10031039.

[9] Jeong, Y.K., et al., Hyperbranched beta-Cyclodextrin Polymer as an Effective Multidimensional Binder for Silicon Anodes in Lithium Rechargeable Batteries. Nano Lett, 2014. 14(2): p. 864-70.

[10] Gowda, S.R., et al., Three-dimensionally engineered porous silicon electrodes for Li ion batteries. Nano Lett, 2012. 12(12): p. 6060-5.

[11] Liu, X.H., et al., Size-Dependent Fracture of Silicon Nanoparticles DuringLithiation. ACs Nano, 2012. 6(2): p. 1522-1531.

[12] Lu, C., et al., Core–shell CNT–Ni–Si nanowires as a high performance anode material for lithium ion batteries. Carbon, 2013. 63: p. 54-60.

[13] Gohier, A., et al., High-rate capability silicon decorated vertically aligned carbon nanotubes for Li-ion batteries. Adv Mater, 2012. 24(19): p. 2592-7.

[14] Lee, K.T. and J. Cho, Roles of nanosize in lithium reactive nanomaterials for lithium ion batteries. Nano Today, 2011. 6(1): p. 28-41.

[15] Tarascon, J. M.; Armand, M. Issues and Challenges Facing Rechargeable Lithium Batteries. Nature 2001, 414 (6861), 359−367. (3) Whittingham, M. S. Materials Challenges Facing Electrical Energy Storage. MRS Bull. 2008, 33 (04), 411−419

[16] Arico, A. S.; Bruce, P.; Scrosati, B.; Tarascon, J.-M.; van Schalkwijk, W. Nanostructured Materials for Advanced Energy Conversion and Storage Devices. Nat. Mater. 2005, 4 (5), 366−377.

[17] Wu, H.; Cui, Y. Designing Nanostructured Si Anodes for High Energy Lithium Ion Batteries. Nano Today 2012, 7 (5), 414−429.

[18] Kovalenko, I.; Zdyrko, B.; Magasinski, A.; Hertzberg, B.; Milicev, Z.; Burtovyy, R.; Luzinov, I.; Yushin, G. A Major Constituent of Brown Algae for Use in High-Capacity Li-Ion Batteries. Science 2011, 334 (6052), 75−79.

[19] Obrovac, M. N.; Christensen, L.; Le, D. B.; Dahn, J. R. Alloy Design for Lithium-Ion Battery Anodes. J. Electrochem. Soc. 2007, 154 (9), A849−A855.

[20] McDowell, M. T.; Lee, S. W.; Nix, W. D.; Cui, Y. 25th Anniversary Article: Understanding the Lithiation of Silicon and Other Alloying Anodes for Lithium-Ion Batteries. Adv. Mater. 2013, 25 (36), 4966−4985.

[21]) Zhang, W.-J. A Review of the Electrochemical Performance of Alloy Anodes for Lithium-Ion Batteries. J. Power Sources 2011, 196 (1), 13−24.

[22] Yi, R.; Dai, F.; Gordin, M. L.; Sohn, H.; Wang, D. Influence of Silicon Nanoscale Building Blocks Size and Carbon Coating on the Performance of Micro-Sized Si−C Composite Li-Ion Anodes. Adv. Energy Mater. 2013, 3 (11), 1507−1515.

[23] Wu, H.; Yu, G.; Pan, L.; Liu, N.; McDowell, M. T.; Bao, Z.; Cui, Y. Stable Li-Ion Battery Anodes by in-Situ Polymerization of Conducting Hydrogel to Conformally Coat Silicon Nanoparticles. Nat. Commun. 2013, 4, 1943

[24] Ma, H.; Cheng, F.; Chen, J. Y.; Zhao, J. Z.; Li, C. S.; Tao, Z. L.; Liang, J. Nest-Like Silicon Nanospheres for High-Capacity Lithium Storage. Adv. Mater. 2007, 19 (22), 4067−4070.

[25] Chan, C. K.; Peng, H.; Liu, G.; McIlwrath, K.; Zhang, X. F.; Huggins, R. A.; Cui, Y. High-Performance Lithium Battery Anodes Using Silicon Nanowires. Nat. Nanotechnol. 2008, 3 (1), 31−35.

[26] Wu, H.; Chan, G.; Choi, J. W.; Ryu, I.; Yao, Y.; McDowell, M. T.; Lee, S. W.; Jackson, A.; Yang, Y.; Hu, L.; Cui, Y. Stable Cycling of Double-Walled Silicon

Nanotube Battery Anodes through SolidElectrolyte Interphase Control. Nat. Nanotechnol. 2012, 7 (5), 310− 315.

[27] Jia, H.; Gao, P.; Yang, J.; Wang, J.; Nuli, Y.; Yang, Z. Novel Three-Dimensional Mesoporous Silicon for High Power Lithium-Ion Battery Anode Material. Adv. Energy Mater. 2011, 1 (6), 1036−1039.

[28] Liu, B.; Wang, X.; Chen, H.; Wang, Z.; Chen, D.; Cheng, Y.-B.; Zhou, C.; Shen, G. Hierarchical Silicon Nanowires-Carbon Textiles Matrix as a Binder-Free Anode for High-Performance Advanced Lithium-Ion Batteries. Sci. Rep. 2013, 3, 1622.

[29] Dellas, N. S.; Liu, B. Z.; Eichfeld, S. M.; Eichfeld, C. M.; Mayer, T. S.; Mohney, S. E. Orientation Dependence of Nickel Silicide Formation in Contacts to Silicon Nanowires. J. Appl. Phys. 2009, 105 (9), 094309.

[30] Hassan, F. M.; Elsayed, A. R.; Chabot, V.; Batmaz, R.; Xiao, X.; Chen, Z. Subeutectic Growth of Single-Crystal Silicon Nanowires Grown on and Wrapped with GrapheneNanosheets:

[31] Nazri GA, Pistoia G (2004) Lithium batteries: science and technology. Kluwer Academic, Boston

[32] Moffat WG (1990) In: Moffatt WG (ed) The handbook of binary phase diagrams. Genium, New York

[33] Boukamp BA, Lesh GC, Huggins RA (1981) J ElectrochemSoc 128:725–729

[34] Chan CK, Peng HL, Liu G, McIlwrath K, Zhang XF, Huggins RA, Cui Y (2008) Nat Nanotechnol 3(1):31–35

[35] Laik B, Eude L, Pereira-Ramos JP, Cojocaru CS, Pribat D, Rouviere E (2008) ElectrochimActa 53(17):5528–5532

[36] Fu Y P; Chen H X; Yang Y (2009) Electrochemistry (Chinese) 15 (1):56-61

[37] Dimov N, Fukuda K, Umeno T, Kugino S, Yoshio M (2003) J Power Sources 114:88–95

[38] Silicon nanowires with and without carbon coating as anode materials for lithium-ion batteries Huixin Chen &Zhixin Dong &Yanpeng Fu & Yong Yang

[39] Nickel-Seeded Silicon Nanowires Grown on Graphene as Anode Material for Lithium-ion Batteries by Abdel Rahman Elsayed.

[40] Lithium Ion Battery Peformance of Silicon Nanowires with Carbon Skin,Timothy D. Bogart,† Daichi Oka,‡ Xiaotang Lu,† MengGu,§ Chongmin Wang,§ and Brian A. Korgel†,*